Electronic Supplementary Material (ESI) for RSC Advances.

Binding Characteristics of Pyrrole-scaffold Hepatitis B Virus Capsid Inhibitors and Identification of Novel Potent Compounds

Tanachote Ruengsatra[1], Arthitaya Meeprasert[1], Eakkaphon Rattanangkool[1], Sirikan Deesiri[1], Jakkrit Srisa[1], Udomsak Udomnilobol[1], Wilasinee Dunkoksung[1], Natthaya Chuaypen[1,2], Rattanaporn Kiatbumrung[1,2], Pisit Tangkijvanich[1,2], Sornkanok Vimolmangkang[3], Khanitha Pudhom[4], and Thomayant Prueksaritanont[1]□□*

[1]Chulalongkorn University Drug Discovery and Drug Development Research Center (Chula4DR), Chulalongkorn University, 254 Phayathai Rd., Pathumwan, Bangkok 10330, Thailand.

[2]Center of Excellence in Hepatitis and Liver Cancer, Department of Biochemistry, Faculty of Medicine; [3]Department of Pharmacognosy and Pharmaceutical Botany; and [4]Department of Chemistry, Faculty of Science, Chulalongkorn University, 1873 Rama 4 Rd, Pathumwan, Bangkok 10330, Thailand.

*Corresponding author. Email address: thomayant.p@pharm.chula.ac.th

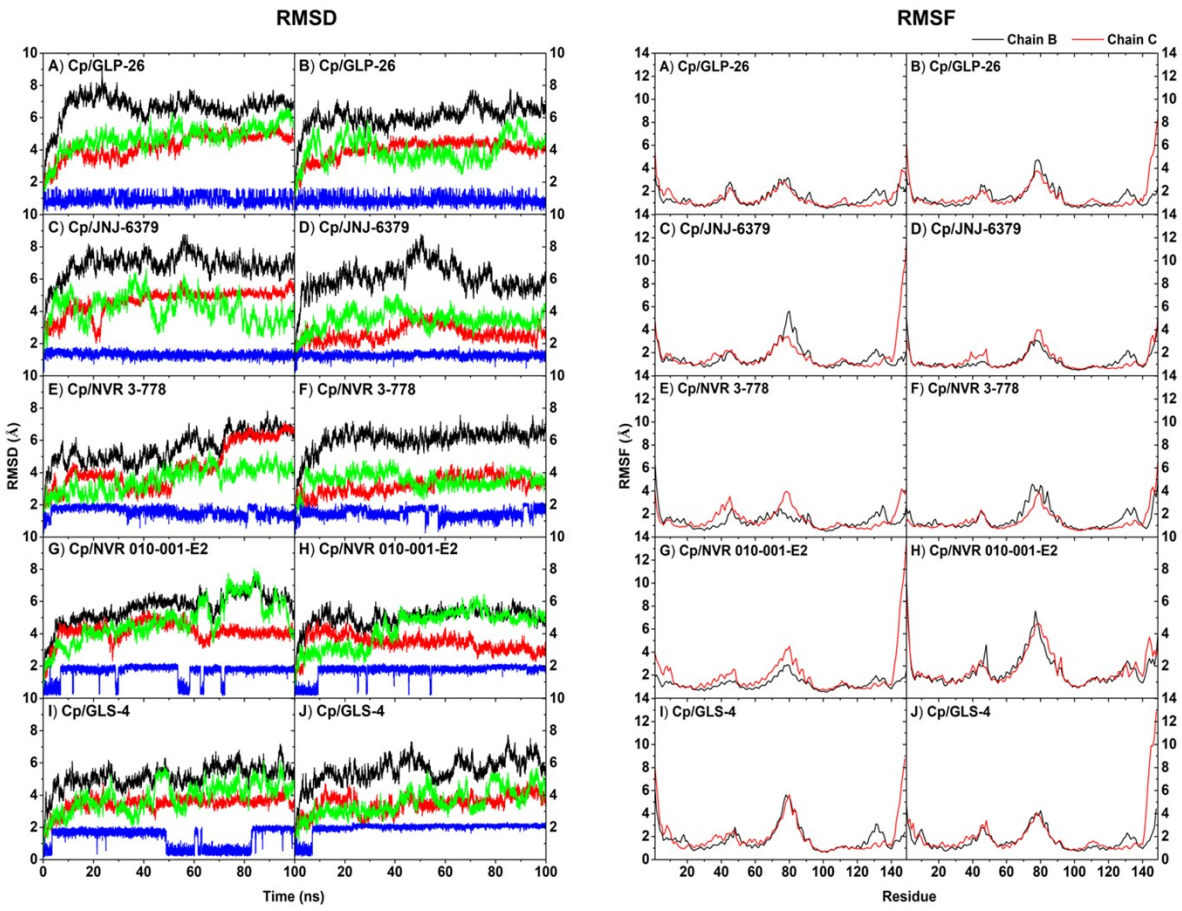

Figure S1. (Left) RMSDs for the heavy atom compared to their starting structures of the HBV Cp dimer complexed with A-B) GLP-26, C-D) JNJ-6379, E-F) NVR 3-778, G-H) NVR 010-001-E2, and I-J) GLS-4 (black = global structure, red = chain B backbone, green = chain C backbone, and blue = ligand). (Right) RMSFs of alpha-carbons in the HBV Cp dimer (black = chain B, red = chain C) complexed with A-B) GLP-26, C-D) JNJ-6379, E-F) NVR 3-778, G-H) NVR 010-001-E2, and I-J) GLS-4 . Two independent simulations are illustrated for each protein-ligand complex.

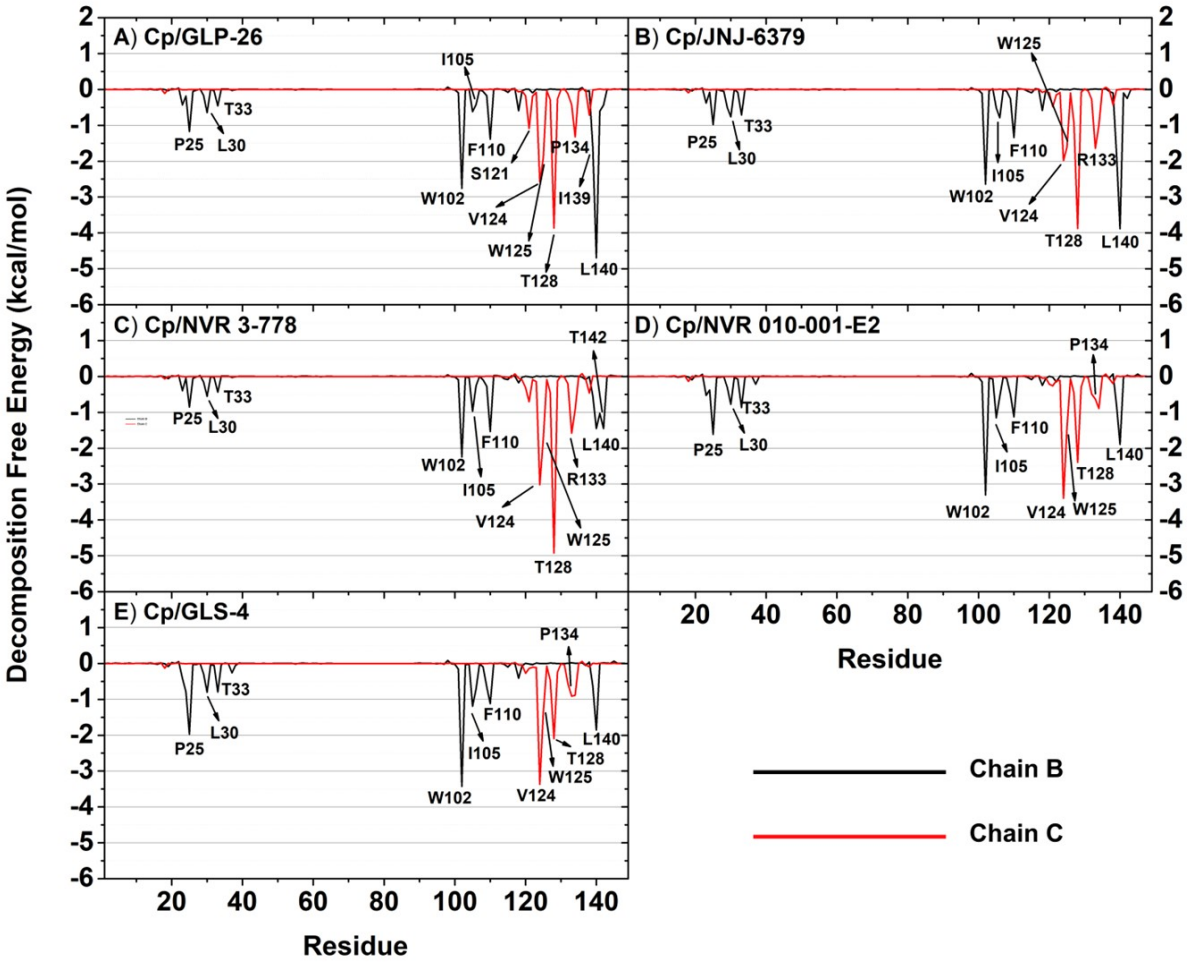

Figure S2. $\Delta G_{bind}^{residue}$ of the HBV Cp dimer complexed with A) GLP-26, B) JNJ-6379, C) NVR 3-778, D) NVR 010-001-E2, and E) GLS-4.

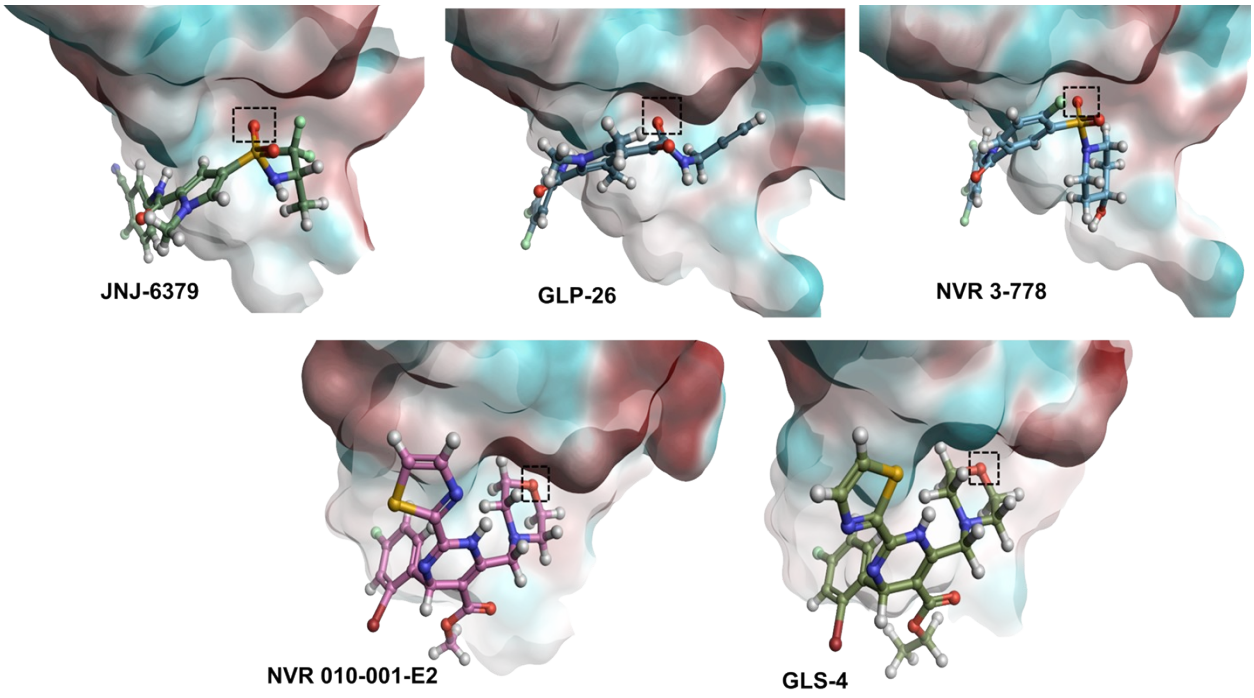

Figure S3. ESP surface of five representative ligand-HBV capsid protein (chain C) complexes (red surface = positive, blue surface = negative). The black rectangle highlights the electronegative atom of the ligands that contacted the positive ESP surface (residues $W125_C$, $R133_C$, and $P134_C$).

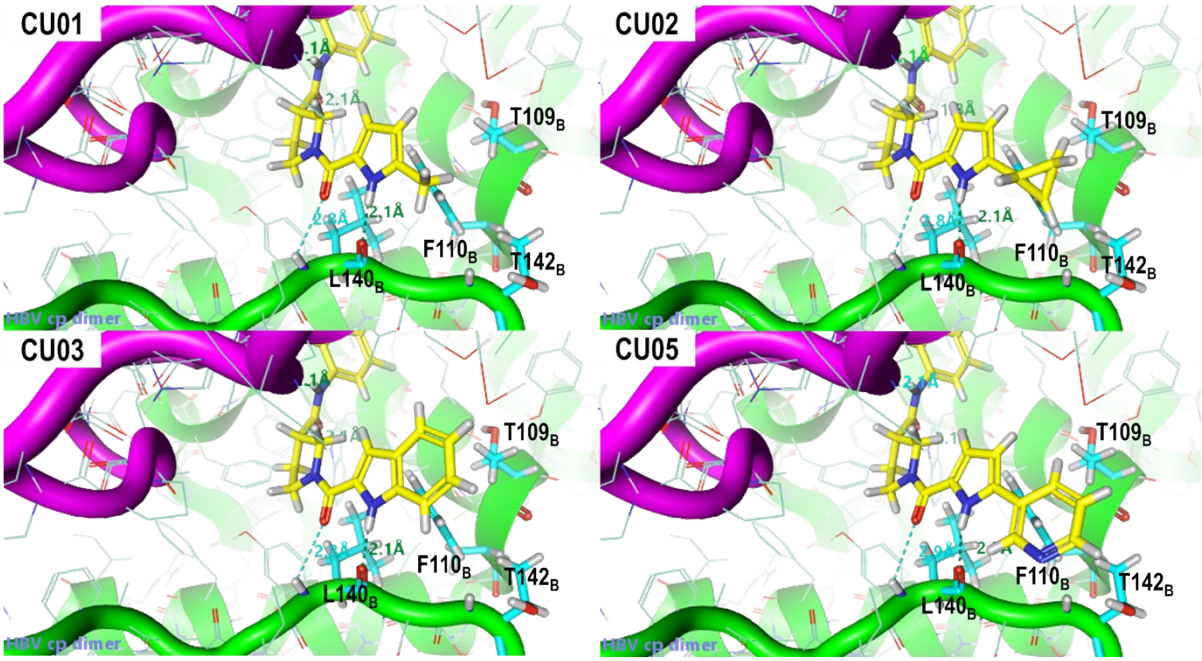

Figure S4. The predicted conformation of CU01-03 and CU05 in HBV capsid dimer interface

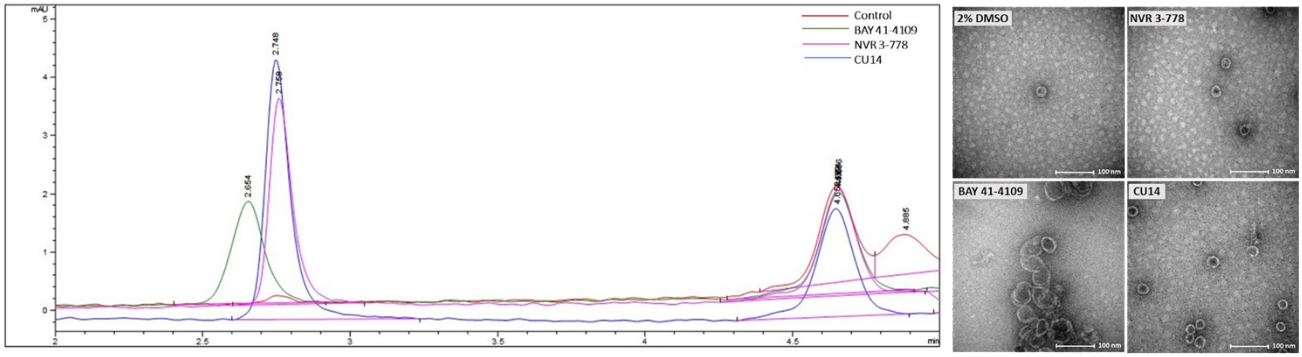

Figure S5. Effects of representative compound CU14 on HBV capsid assembly, determined by size exclusion chromatography (SEC, A) and transmission electron microscopy (TEM, B).

Table S1. $\Delta G_{bind}^{residue}$ (kcal/mol) of the essential binding residues in HBV Cp dimer in complexation with five representative inhibitors.

Residues	GLP-26		JNJ-6379		NVR 3-778		NVR 010-001-E2		GLS-4		Binding region
	Nonpolar	Polar	Nonpolar	Polar	Nonpolar	Polar	Nonpolar	Polar	Nonpolar	Polar	
$P25_B$	-1.288	0.117	-1.086	0.104	-1.025	0.169	-1.715	0.104	-2.064	0.092	L1
$W102_B$	-1.320	-1.439	-1.783	-0.857	-1.499	-0.747	-2.323	-0.977	-2.269	-1.155	L1-L2
$I105_B$	-0.674	0.053	-0.682	0.164	-0.736	-0.231	-1.040	-0.113	-1.141	-0.053	L1
$F110_B$	-1.539	0.155	-1.724	0.385	-1.839	0.306	-1.347	0.221	-1.372	0.251	L2
$S121_C$	-1.105	0.021	-0.908	0.425	-1.131	0.425	-0.605	0.344	-0.369	0.233	L3
$V124_C$	-2.625	0.055	-2.232	0.246	-2.839	-0.177	-3.373	-0.023	-3.427	0.062	L1
$W125_C$	-1.630	-0.285	-1.584	-0.024	-1.843	0.102	-1.389	-0.029	-1.321	-0.054	L3
$T128_C$	-2.753	-1.107	-2.152	-1.726	-2.337	-2.581	-2.356	-0.037	-2.167	0.072	L1-L2
$R133_C$	-0.743	0.315	-1.107	-0.533	-1.013	-0.565	-0.815	0.183	-1.022	0.112	L3
$P134_C$	-1.536	0.218	-1.114	0.114	-0.984	0.059	-0.981	0.086	-0.942	0.055	L3
$I139_B$	-1.293	-0.339	-1.206	-0.606	-0.571	0.025	-0.900	0.094	-0.758	0.120	L3
$L140_B$	-3.075	-1.617	-2.719	-1.160	-2.704	1.254	-2.567	0.671	-2.594	0.738	L2-L3
$S141_B$	-0.920	0.311	-0.768	0.671	-0.915	-0.115	-0.166	0.149	-0.161	0.164	L3
$T142_B$	-0.472	0.033	-0.467	0.219	-0.199	-1.251	-0.028	0.059	-0.040	0.061	L3
$W125_c$, $R133_C$, and $P134_C$	-3.91	0.25	-3.81	-0.443	-3.84	-0.40	-3.19	0.24	-3.29	0.113	L3 small pocket

Polar ($\Delta E_{ele} + \Delta G_{polar}$) and nonpolar ($\Delta E_{vdW} + \Delta G_{nonpolar}$) energy contributions were analyzed for selected residues.

METABOLITE IDENTIFICATION

Identification of metabolic soft spots using high resolution mass spectrometry

The metabolite identification was conducted using the AB Sciex X500B Q-TOF LC-MS/MS system. The samples were chromatographically separated using the Exion LC AD100 system with a Phenomenex Kinetex® C-18, 1.7 µm, 50×2.1 mm analytical column. The mobile phases consisted of water and acetonitrile, both fortified with 0.1% formic acid, and were used as phase A and B, respectively. The flow rate was set at 0.4 mL/min using a 2-step linear gradient from 2% to 65% B for 4 min, followed by ramping to 95% for 0.5 min. The Turbo V™ ion source was operated in the electrospray positive ionization mode under following conditions: curtain gas at 40 psi, heating gas 1 at 40 psi, nebulizing gas 2 at 40 psi, temperature at 450 °C, ion spray voltage floating at 4.5 kV, and declustering potential at 80 V. Mass calibration was performed every 5 sample injections using a standard calibration solution. The TOF MS scan and product ion (MS/MS) spectra were acquired for the m/z range 50-800.

Dynamic background subtraction and the mass defect filter (MDF) function were enabled. The MDF window was set at ±40 mDa, and the mass range was set as ±40 Da around the m/z value of the parent ion. An information-dependent data acquisition (IDA) method was used for triggering MS/MS acquisition for the top 6 intense ions using CE spread at 35±15 V. The data were processed and interpreted using SCIEX OS version 1.6 and MetabolitePilot™ version 2.0 software (AB SCIEX, MA, USA).

Ion chromatograms of parent CU02 and its metabolites

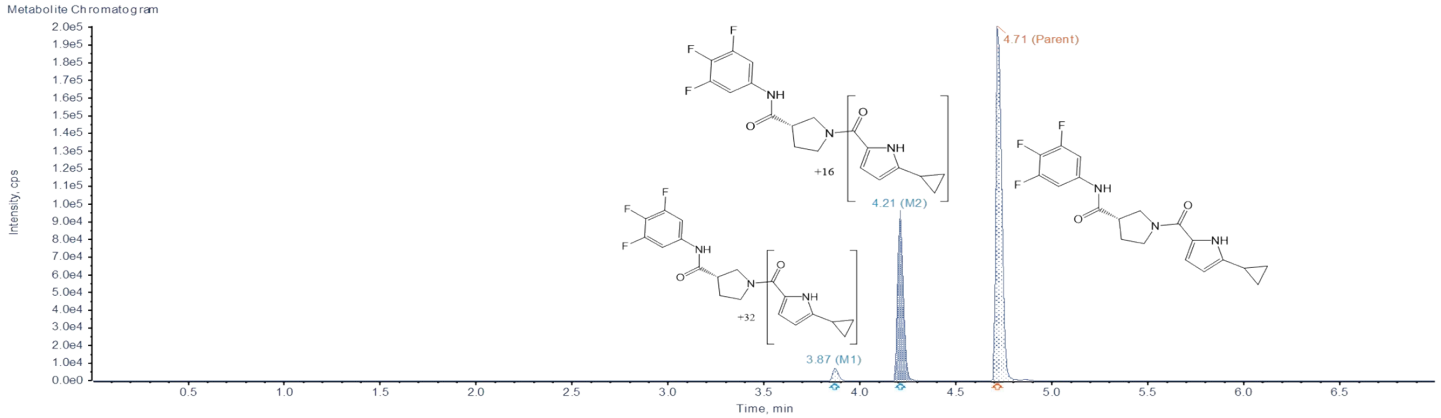

Structures and fragmentation spectra of parent CU02 and its metabolites

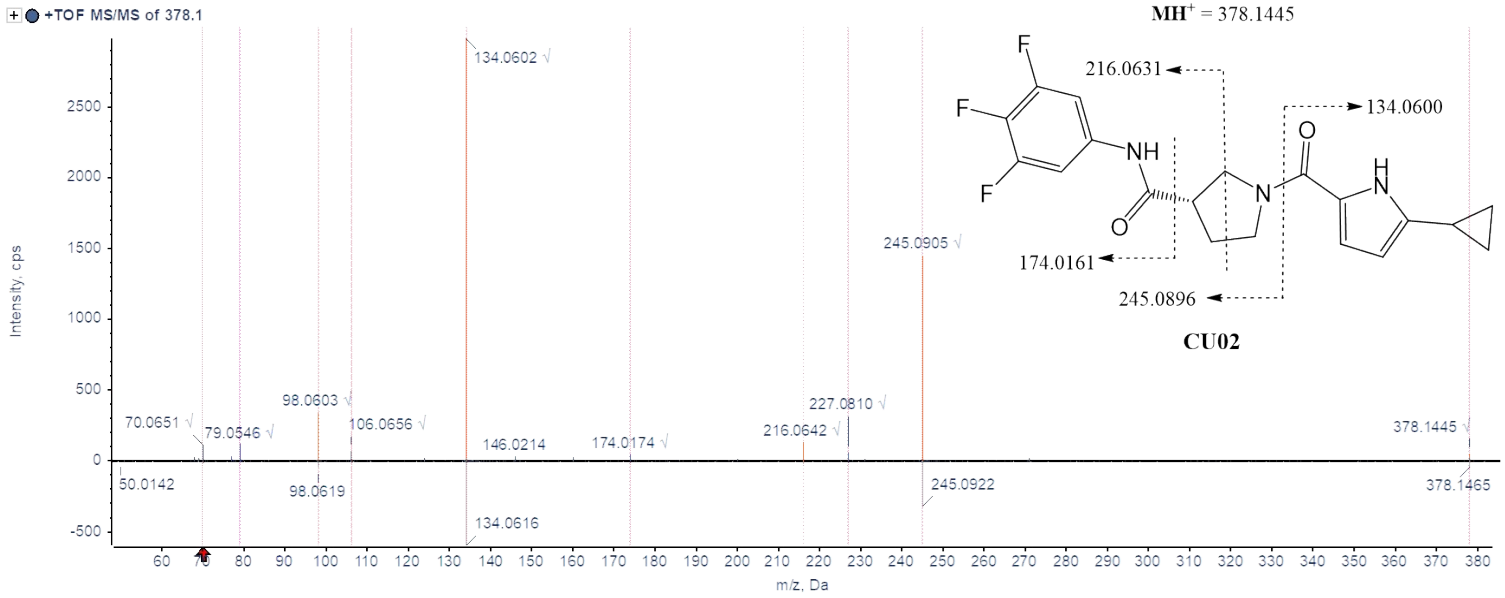


+TOF MS/MS of 410.1
Intensity, cps
m/z, Da
245.0908 √
98.0608 √
70.0650 √
69.0464
70.0707
120.0143 √
148.0407 √
136.0394
166.0516 √
165.0734
166.0354
216.0627 √
227.0809
254.9900
271.0750
277.0872
296.8131
410.1933 x
410.1385 x
410.2678
69.0464
98.0514
98.0619
134.0616
245.0922
378.1465
MH+ = 410.1322
216.0631
166.0499
-H2O
148.0393
245.0896
+2O
CU02 - M1

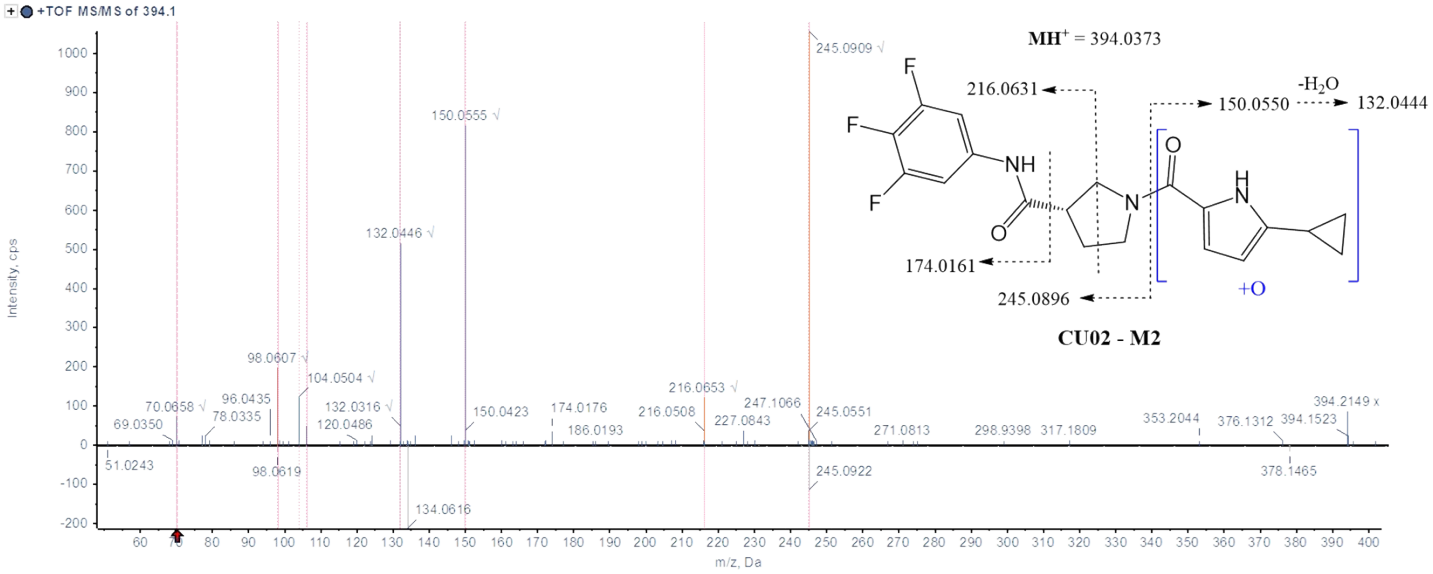
+TOF MS/MS of 394.1
Intensity, cps
m/z, Da
245.0909 √
150.0555 √
132.0446 √
98.0607 √
104.0504 √
70.0658 √
96.0435
78.0335
69.0350
132.0316 √
120.0486
150.0423
174.0176
186.0193
216.0653 √
216.0508
247.1066
227.0843
245.0551
271.0813
298.9398
317.1809
353.2044
376.1312
394.1523
394.2149 x
51.0243
98.0619
134.0616
245.0922
378.1465
MH+ = 394.0373
216.0631
150.0550
-H2O
132.0444
174.0161
245.0896
+O
CU02 - M2

Ion chromatograms of parent CU03 and its metabolites

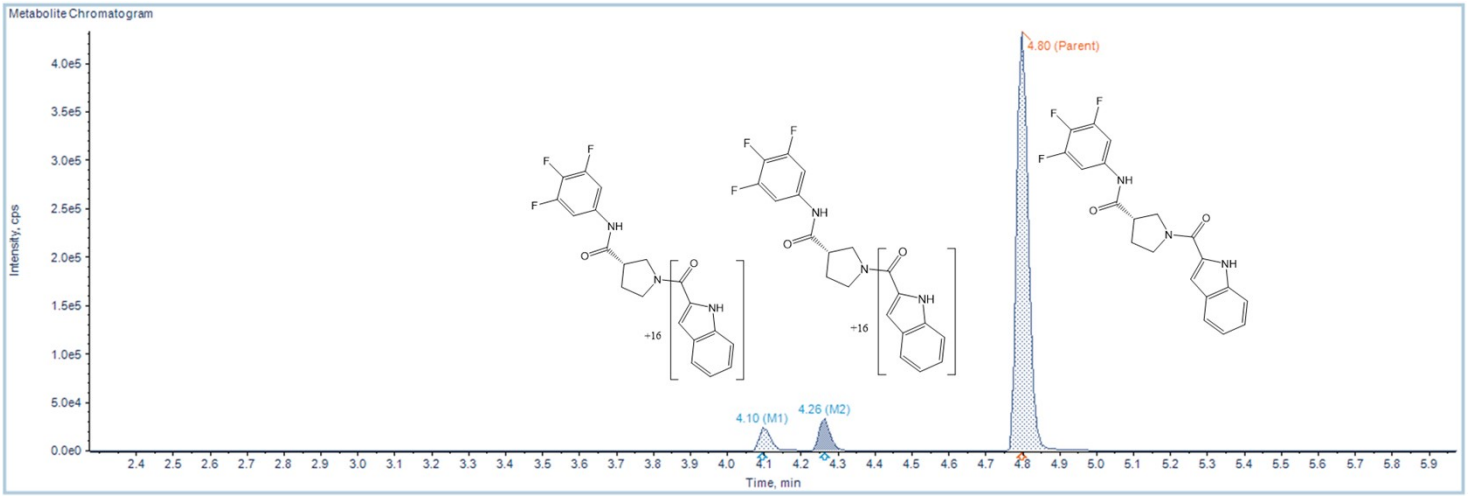

Structures and fragmentation spectra of parent CU03 and its metabolites

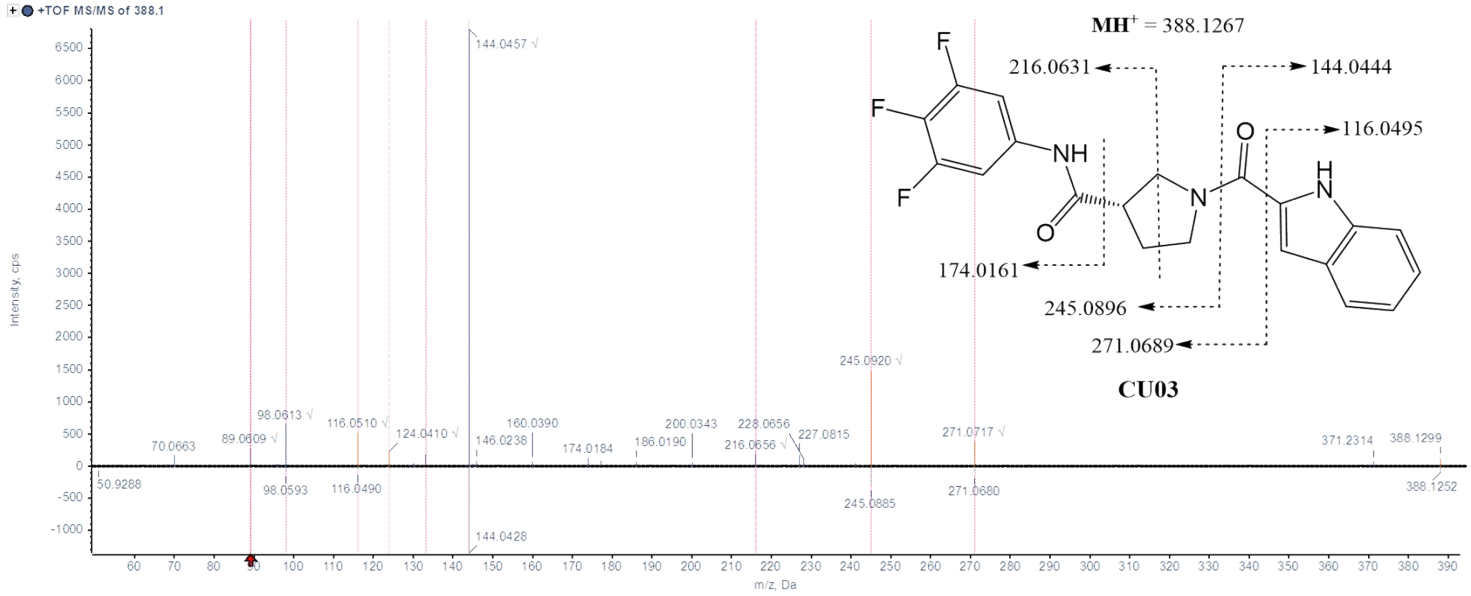

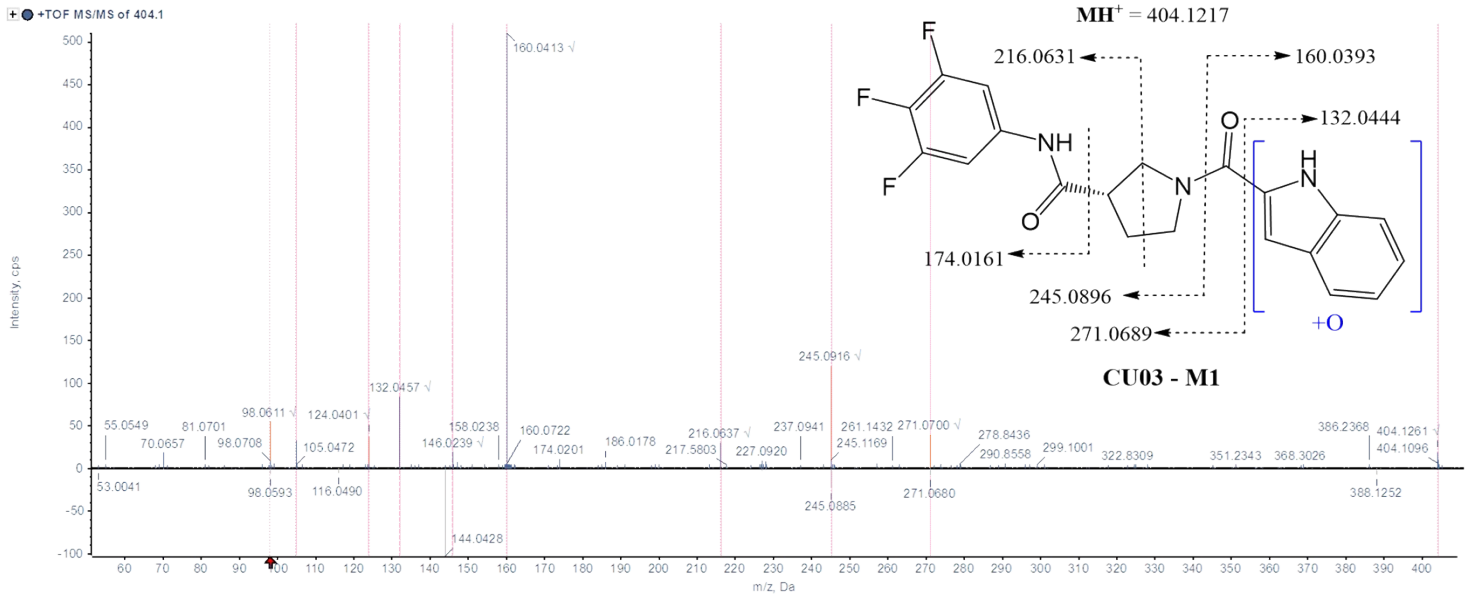
+TOF MS/MS of 404.1
Intensity, cps
m/z, Da
160.0413
132.0457
245.0916
98.0611
124.0401
55.0549
81.0701
70.0657
98.0708
105.0472
158.0238
146.0239
160.0722
174.0201
186.0178
216.0637
217.5803
227.0920
237.0941
261.1432
245.1169
271.0700
278.8436
290.8558
299.1001
322.8309
351.2343
368.3026
386.2368
404.1261
404.1096
53.0041
98.0593
116.0490
144.0428
245.0885
271.0680
388.1252
MH+ = 404.1217
216.0631
160.0393
132.0444
174.0161
245.0896
271.0689
+O
CU03 - M1

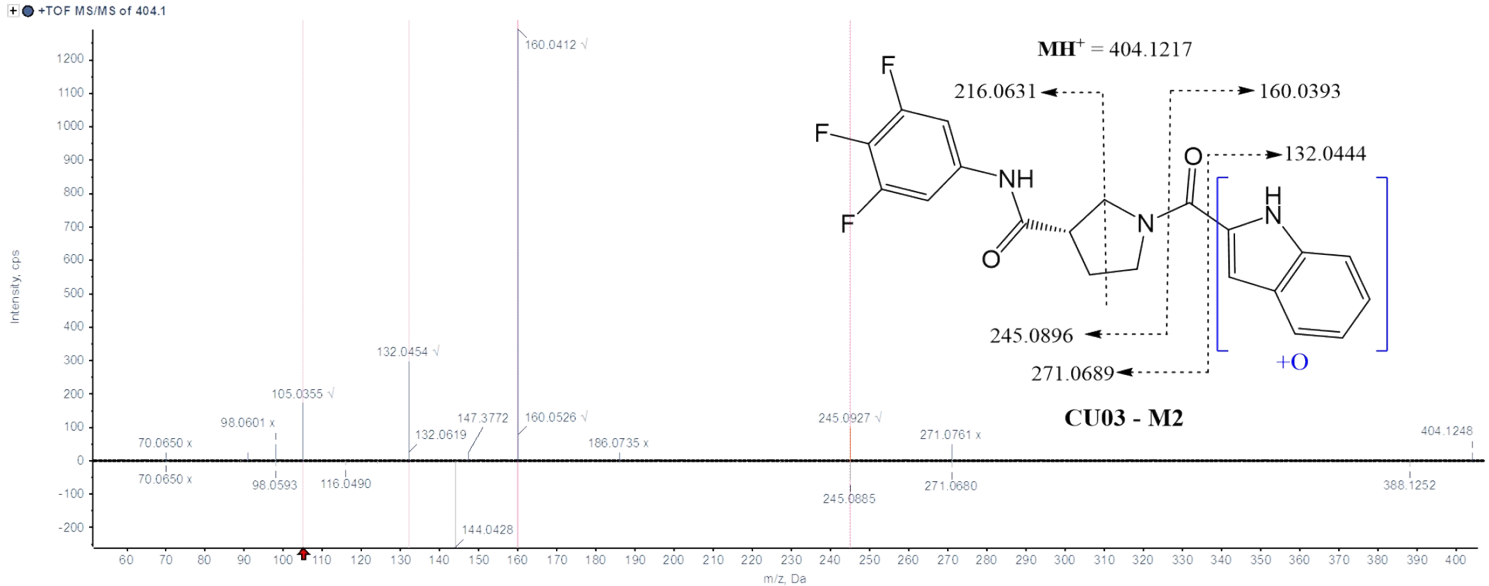
+TOF MS/MS of 404.1
Intensity, cps
m/z, Da
160.0412
132.0454
105.0355
98.0601 x
147.3772
132.0619
160.0526
70.0650 x
186.0735 x
245.0927
271.0761 x
404.1248
70.0650 x
98.0593
116.0490
144.0428
245.0885
271.0680
388.1252
MH+ = 404.1217
216.0631
160.0393
132.0444
245.0896
271.0689
+O
CU03 - M2

NMR SPECTRUM OF SYNTHESIZED COMPOUNDS

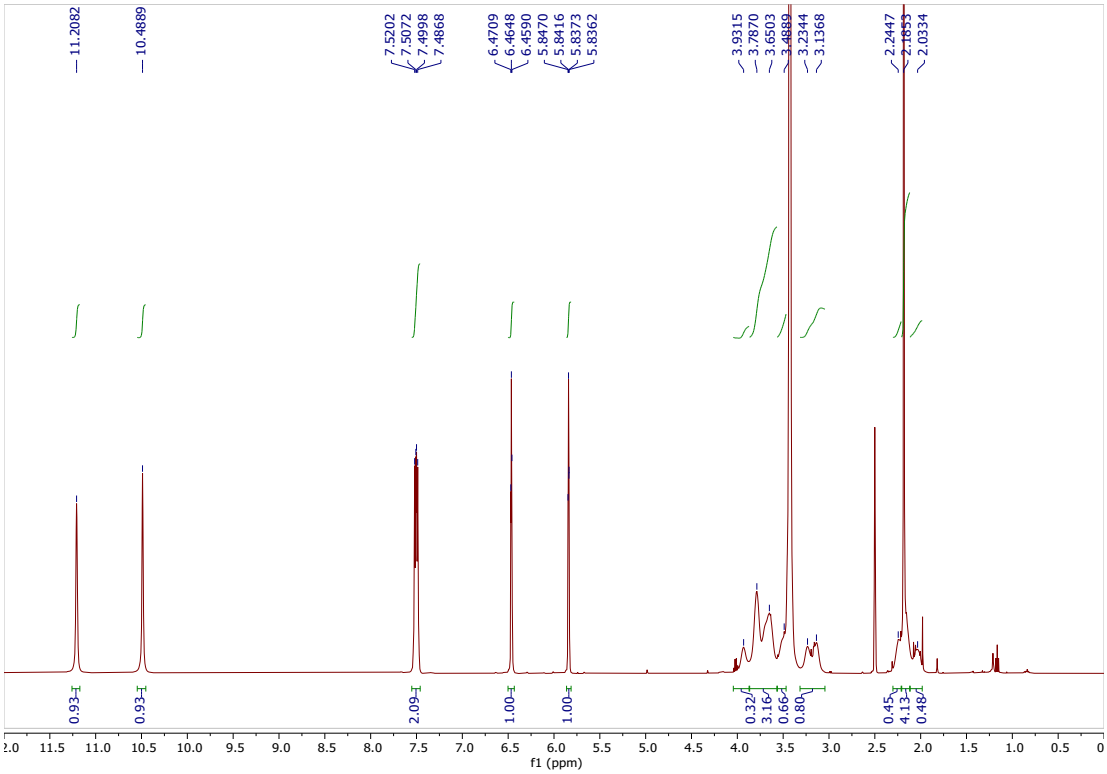

^{1}H NMR spectrum of **CU01** (DMSO-d_6)

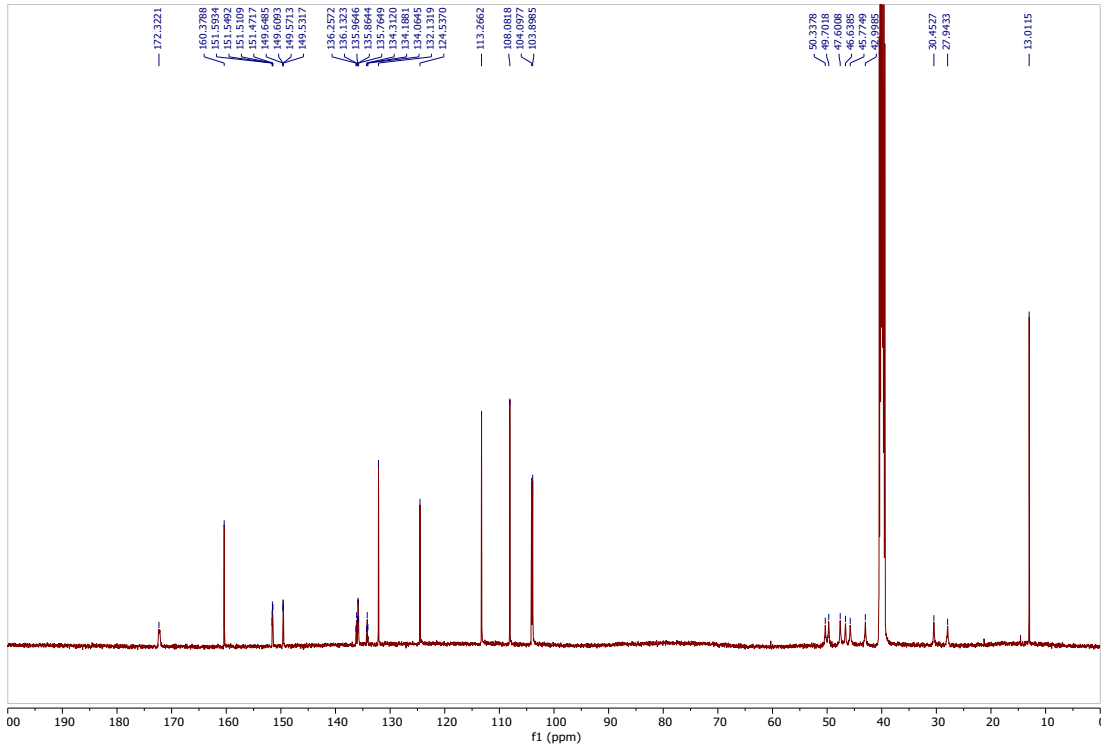

^{13}C NMR spectrum of **CU01** (DMSO-d_6)

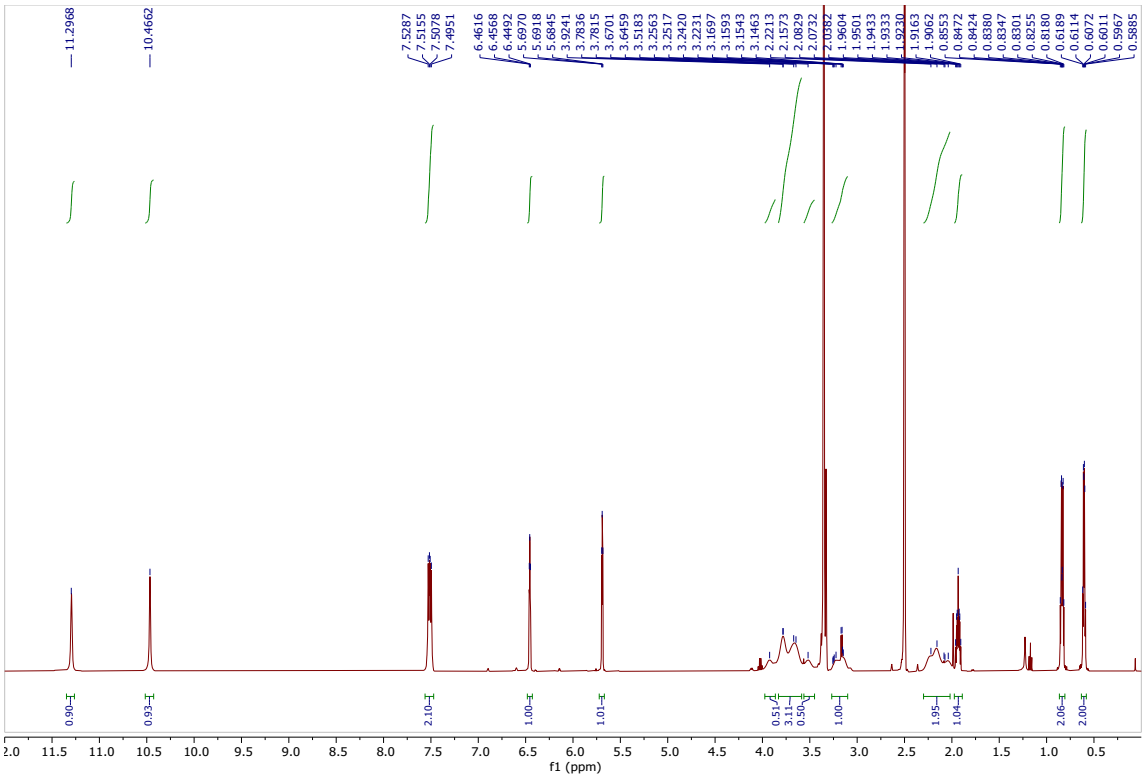

^{1}H NMR spectrum of **CU02** (DMSO-d_6)

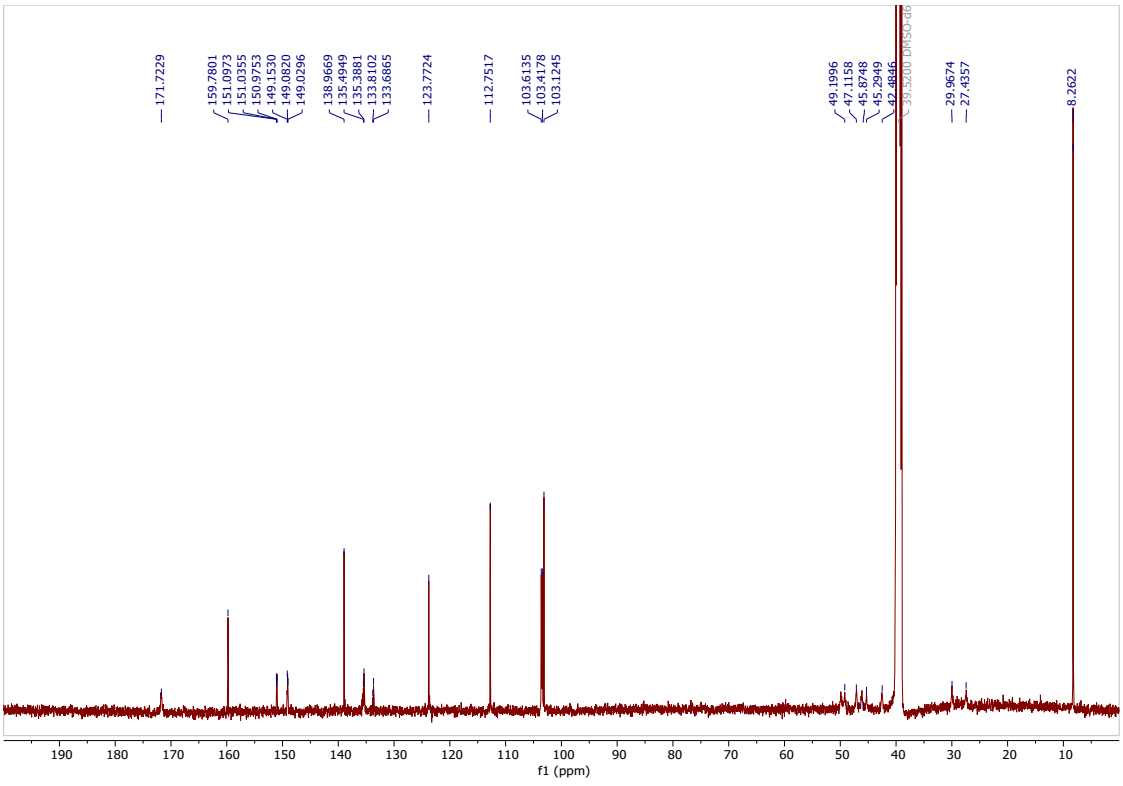

^{13}C NMR spectrum of **CU02** (DMSO-d_6)

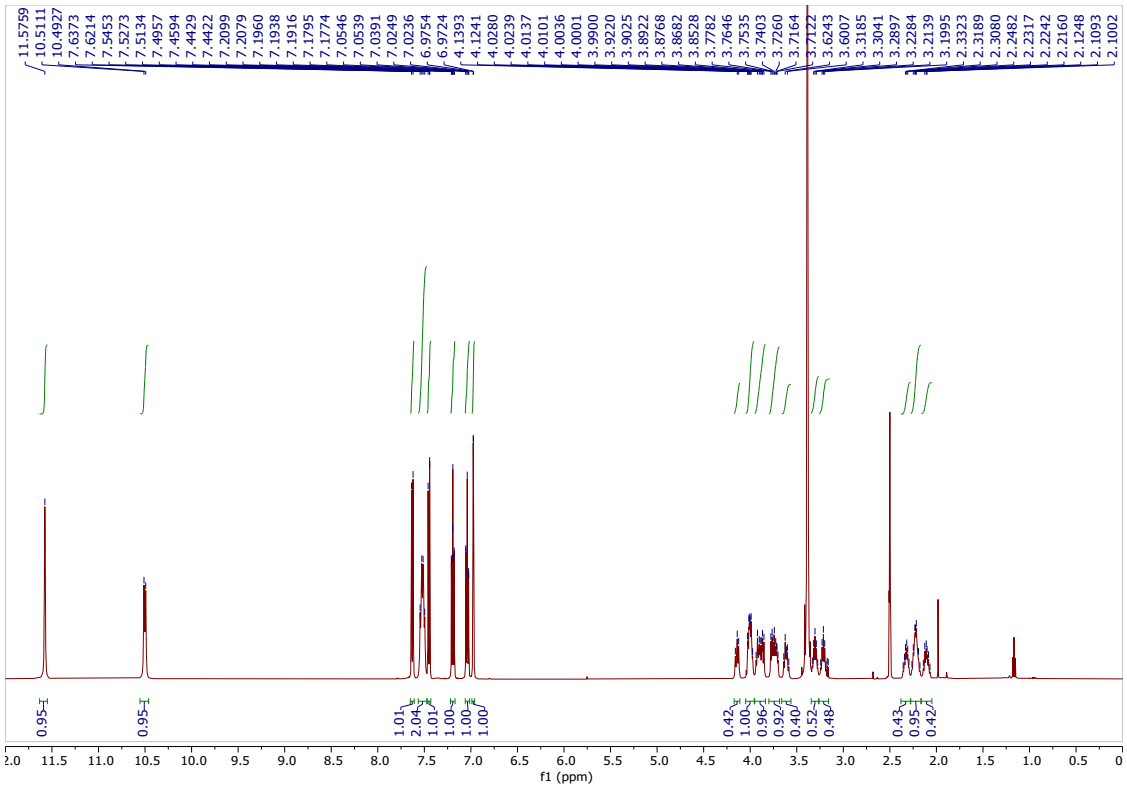

^{1}H NMR spectrum of **CU03** (DMSO-d_6)

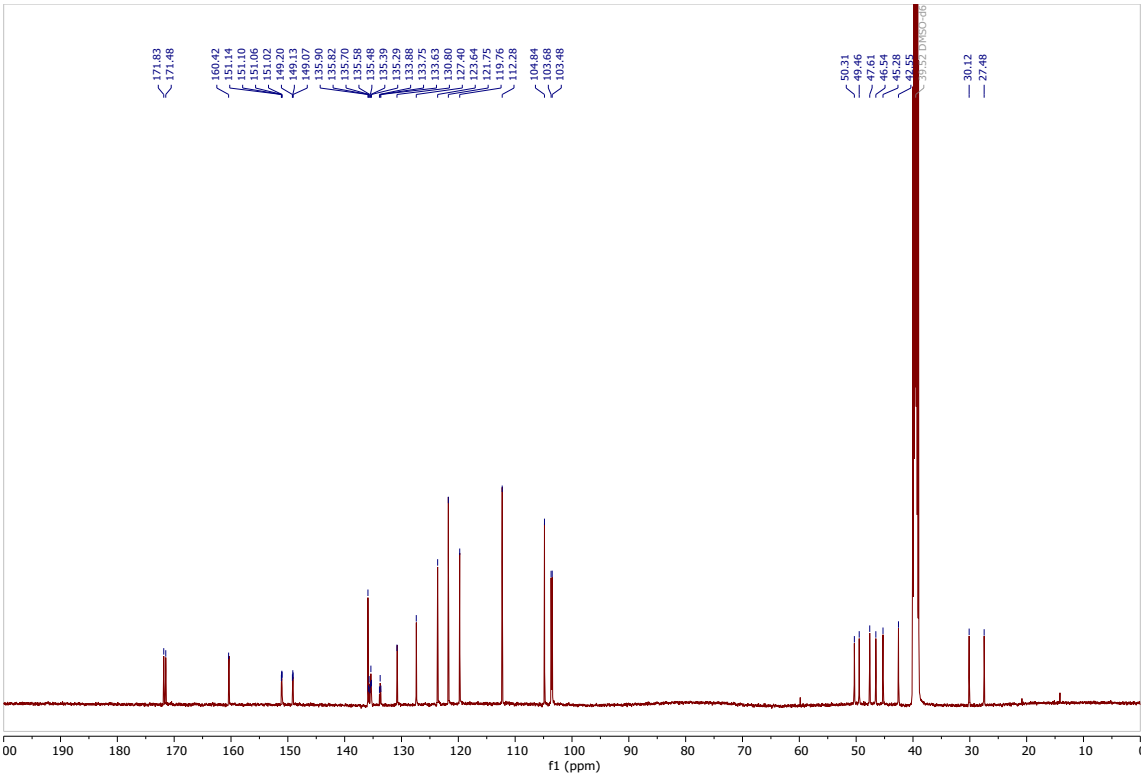

^{13}C NMR spectrum of **CU03** (DMSO-d_6)

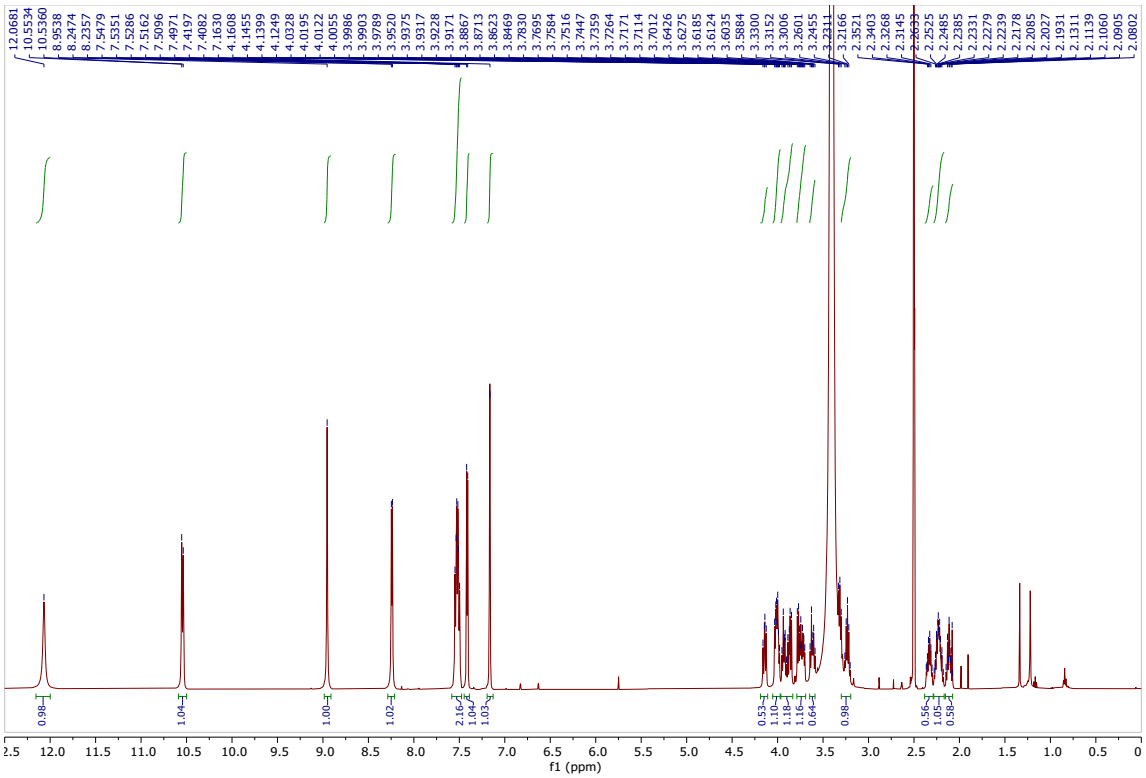

^{1}H NMR spectrum of **CU04** (DMSO-d_6)

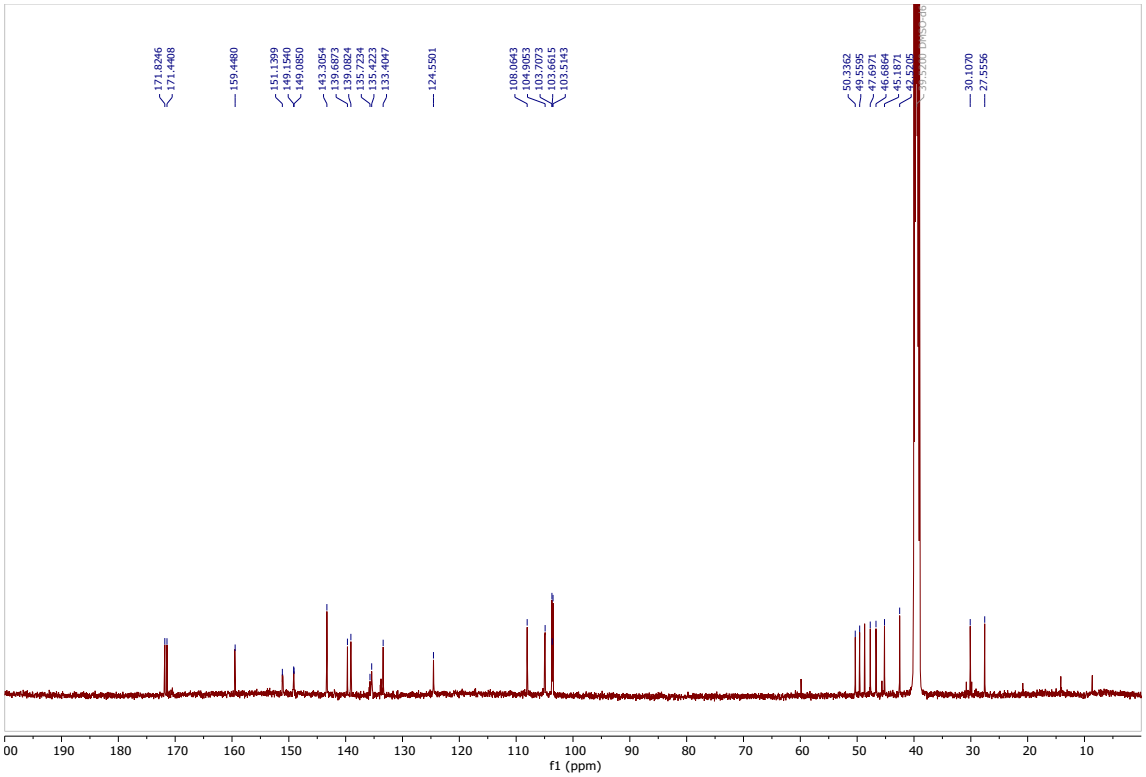

^{13}C NMR spectrum of **CU04** (DMSO-d_6)

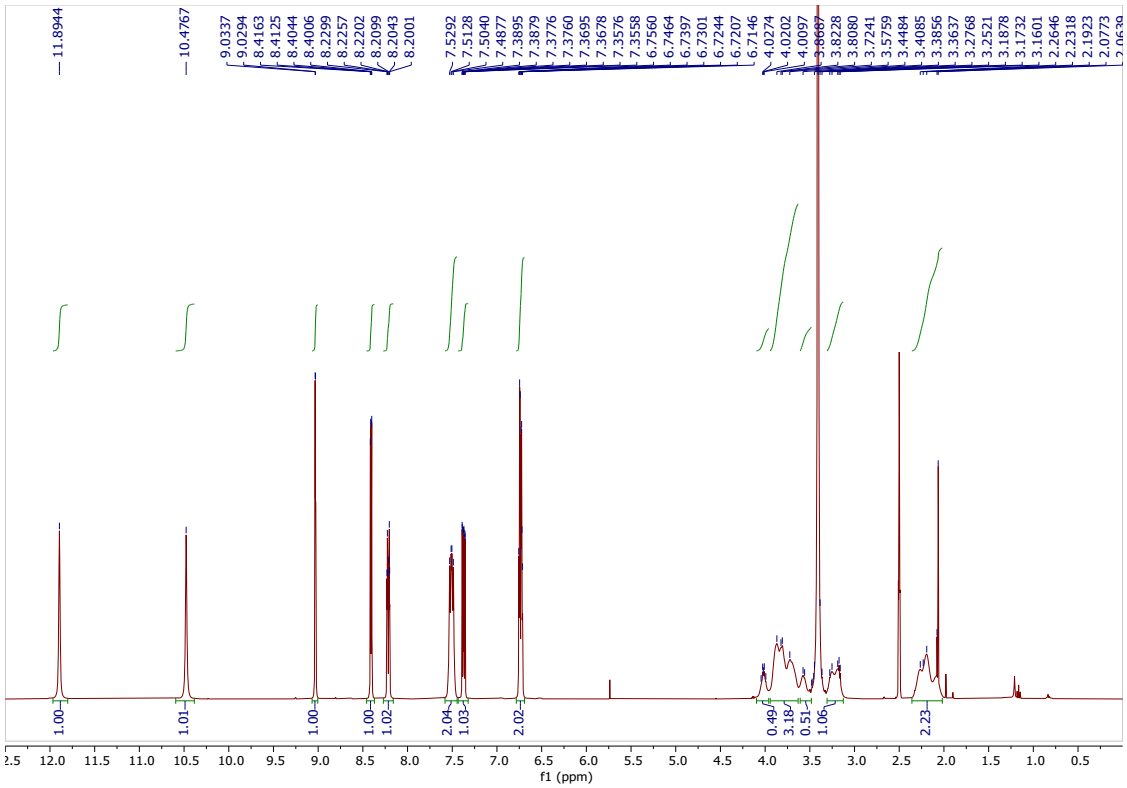

^{1}H NMR spectrum of **CU05** (DMSO-d_6)

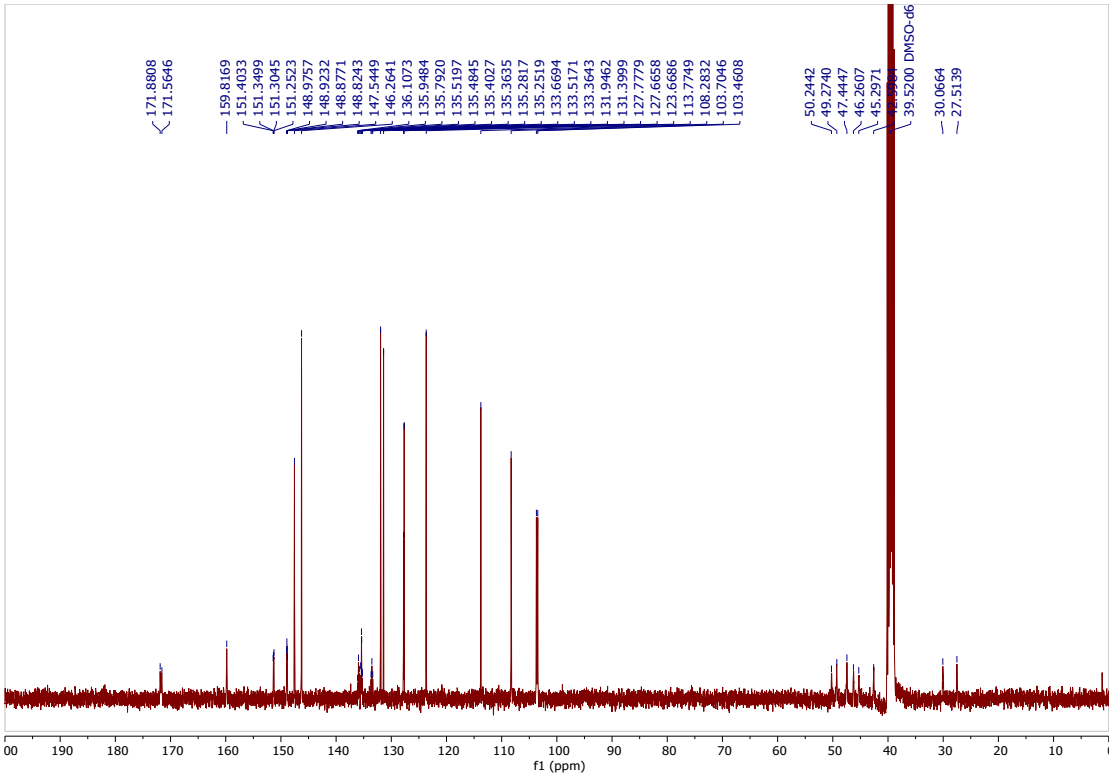

^{13}C NMR spectrum of **CU05** (DMSO-d_6)

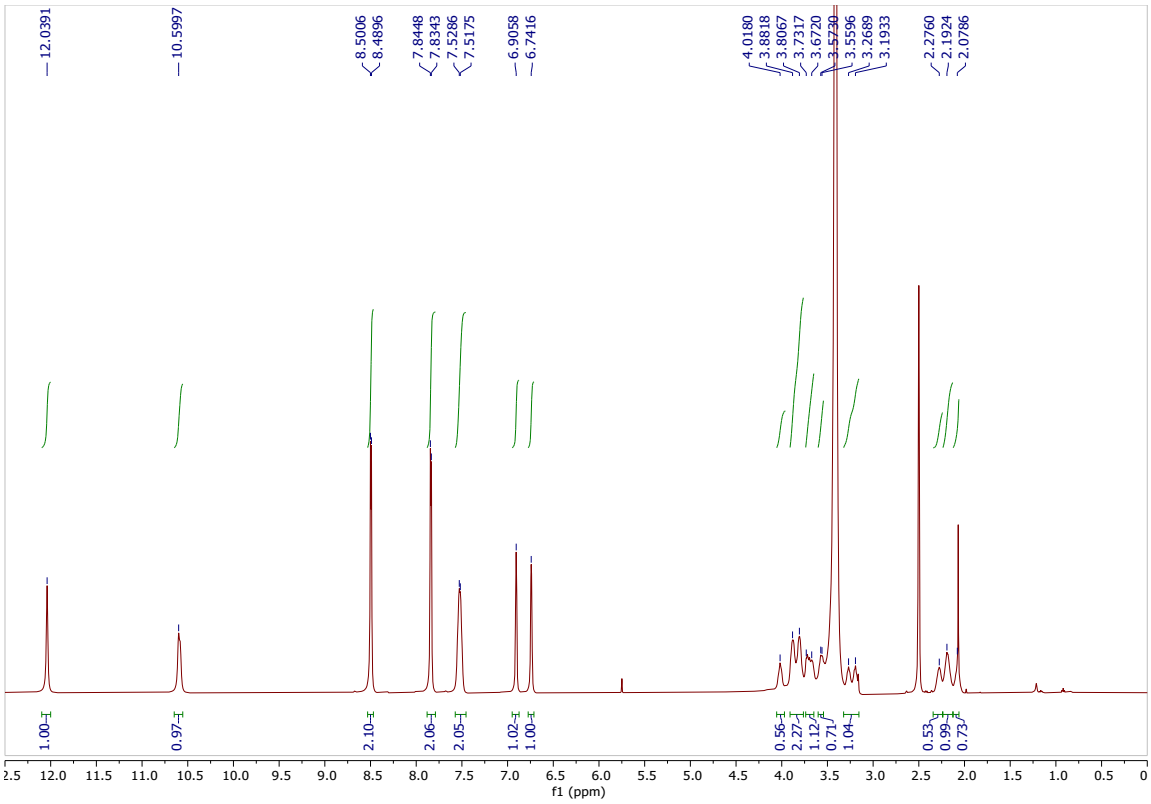

^{1}H NMR spectrum of **CU06** (DMSO-d_6)

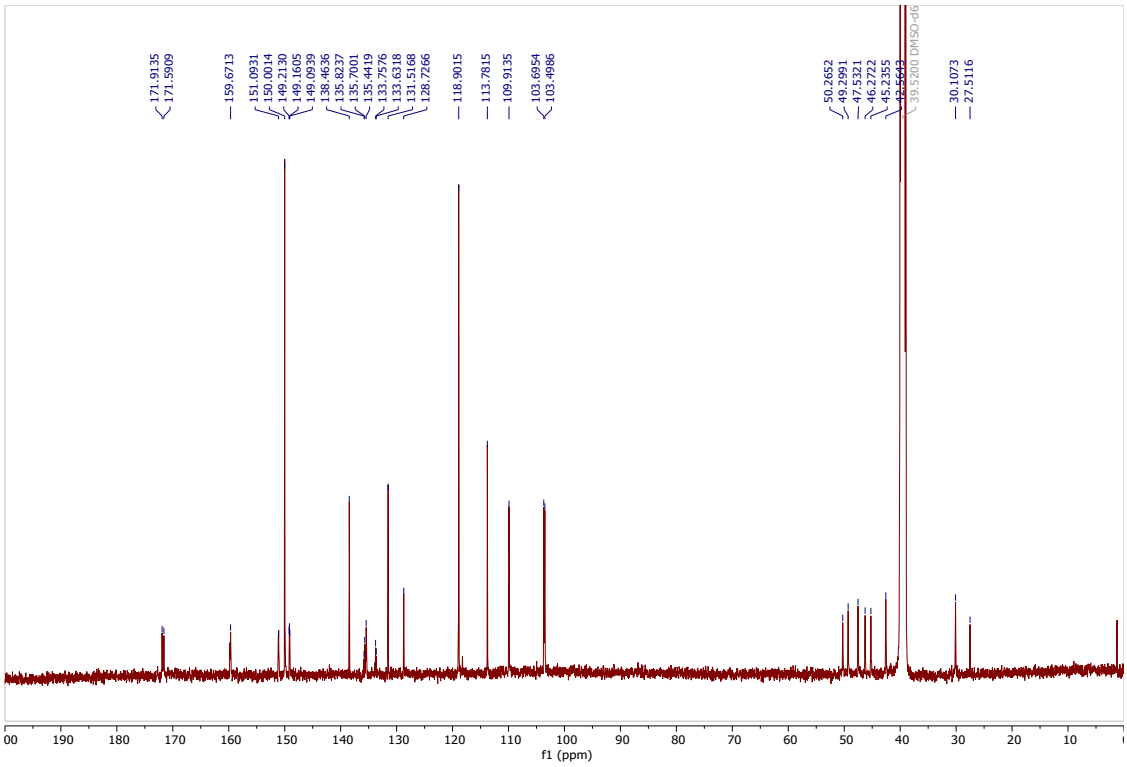

^{13}C NMR spectrum of **CU06** (DMSO-d_6)

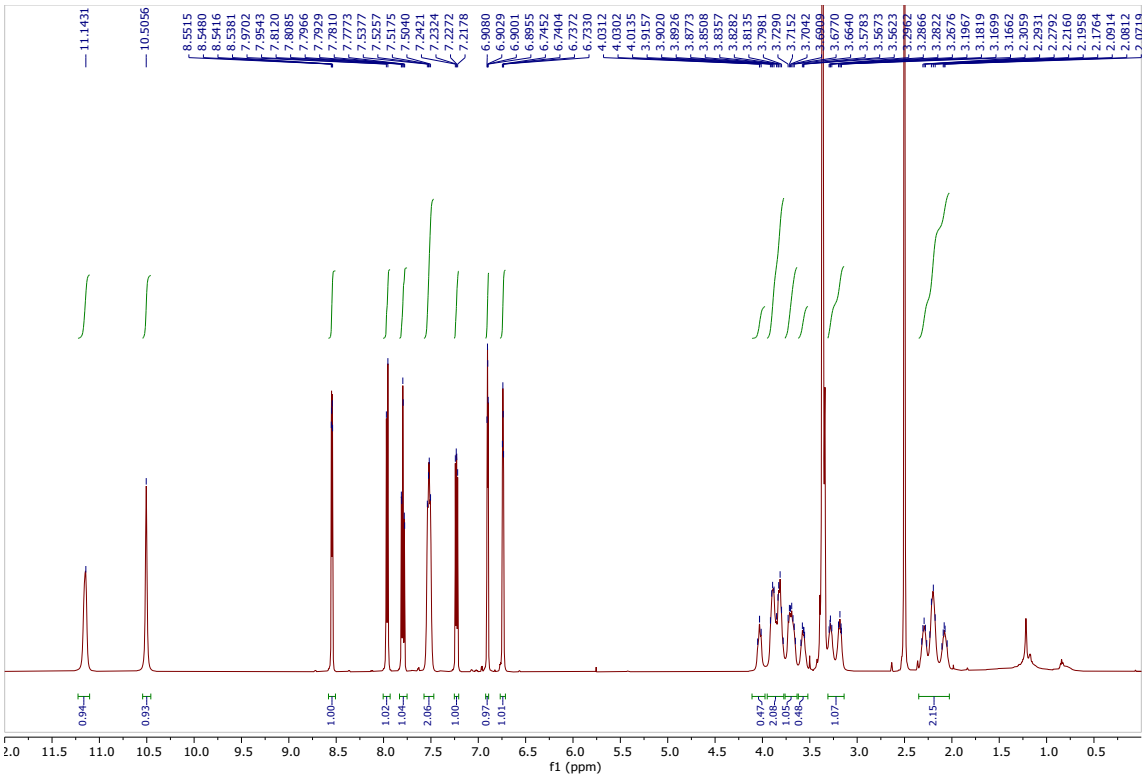

^{1}H NMR spectrum of **CU07** (DMSO-d_6)

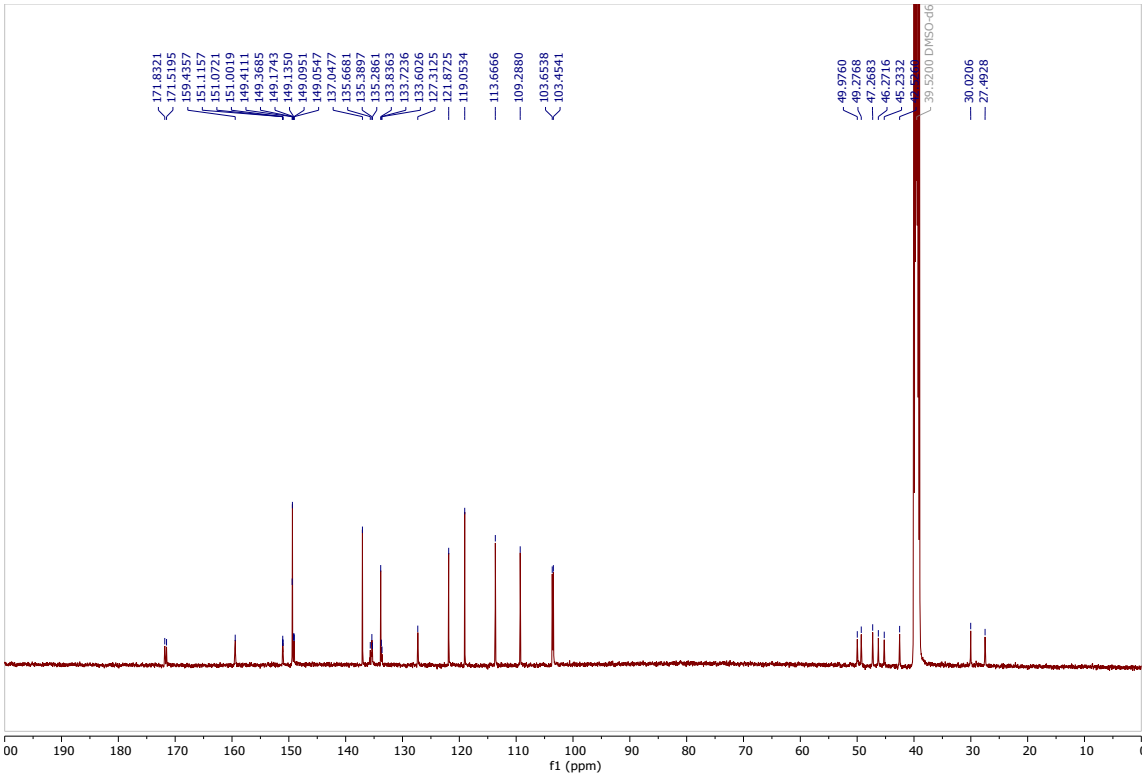

^{13}C NMR spectrum of **CU07** (DMSO-d_6)

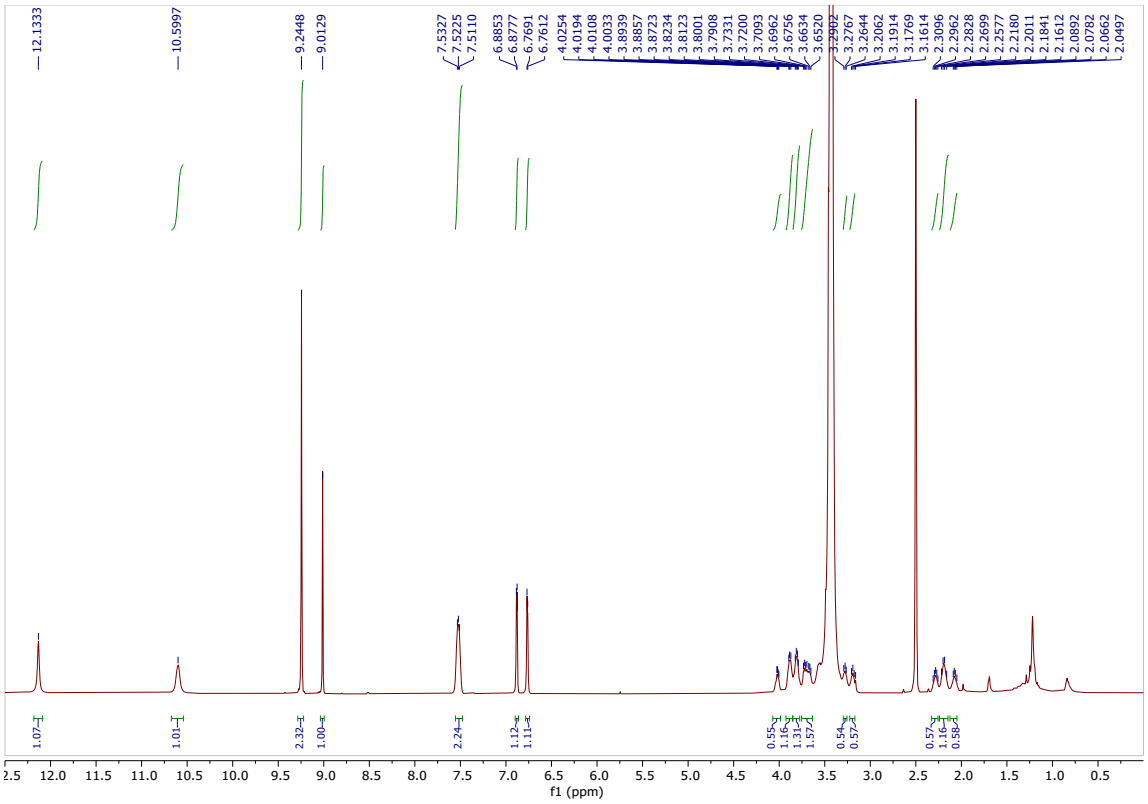

^{1}H NMR spectrum of **CU08** (DMSO-d_6)

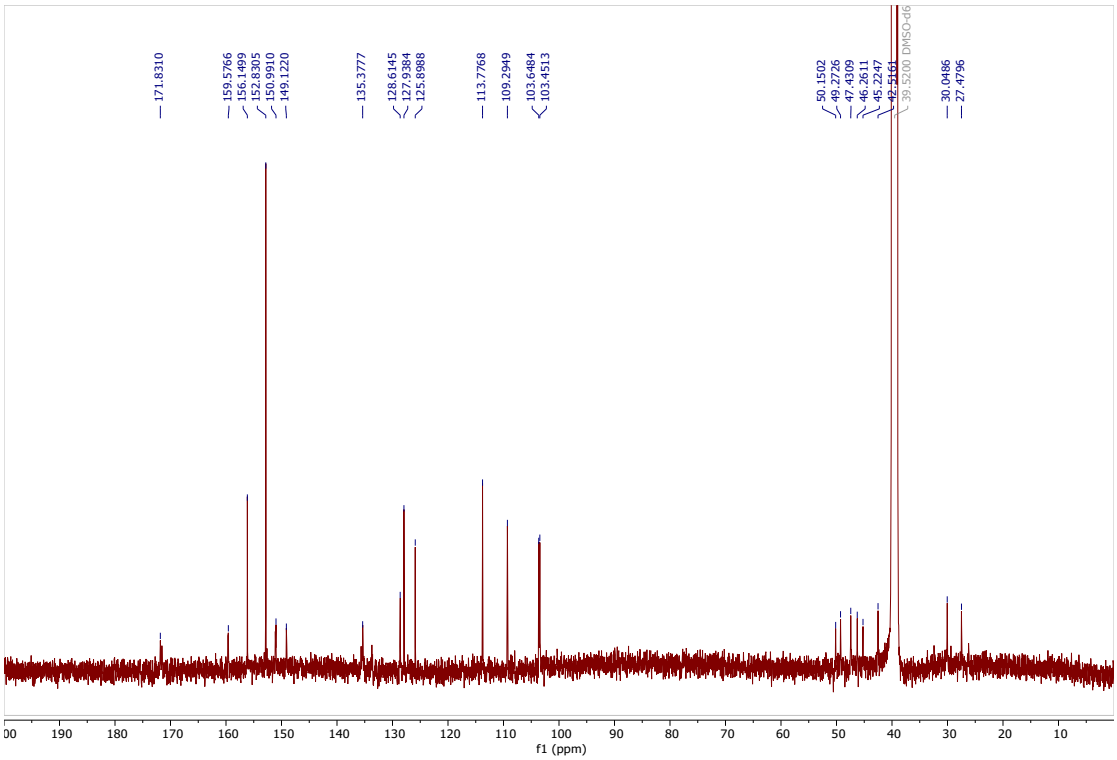

^{13}C NMR spectrum of **CU08** (DMSO-d_6)

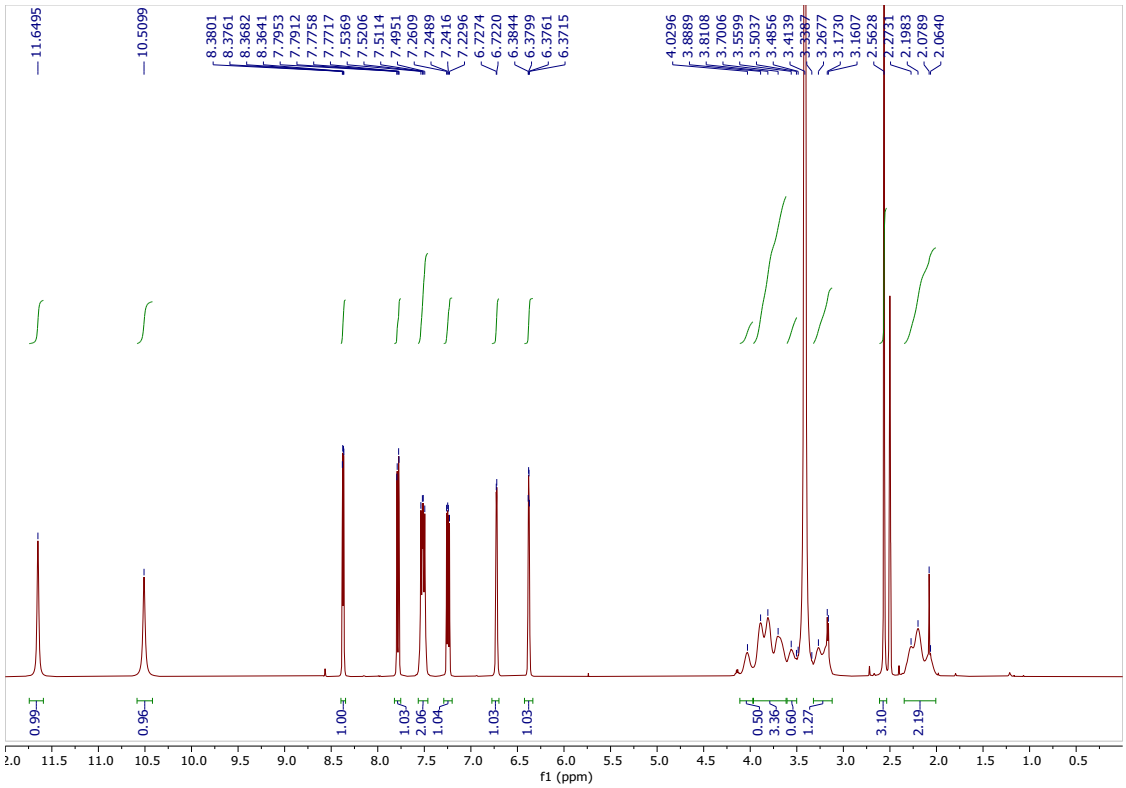

^{1}H NMR spectrum of **CU09** (DMSO-d_6)

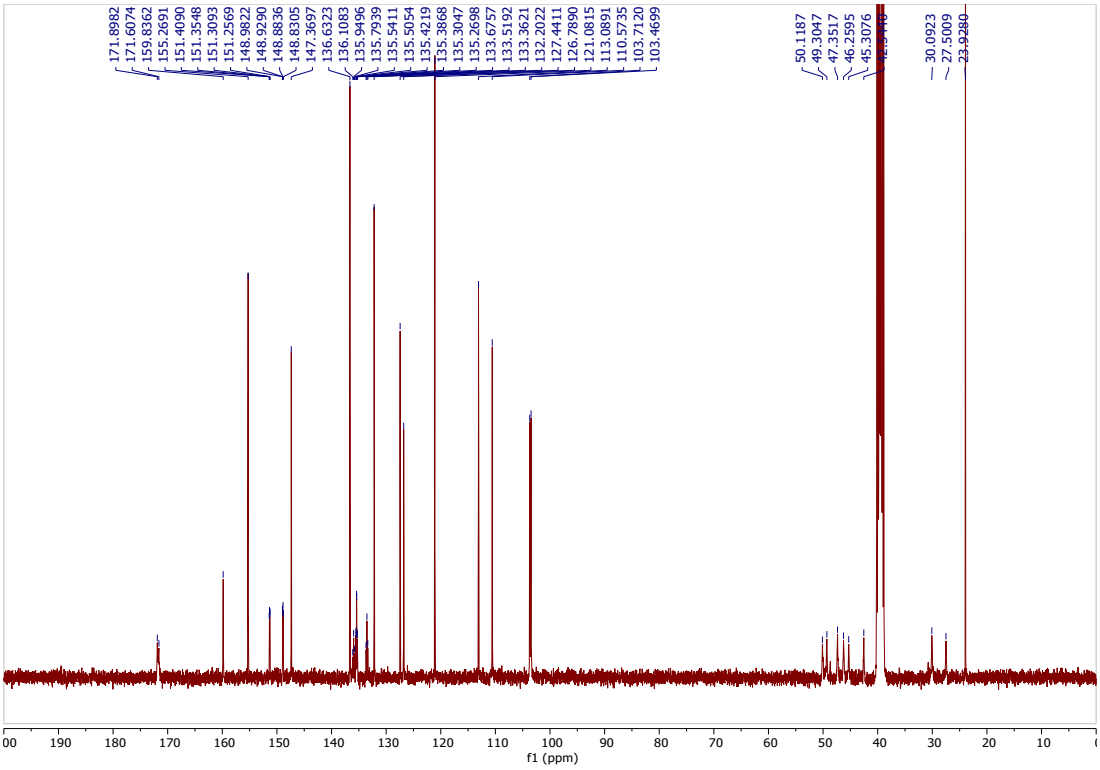

^{13}C NMR spectrum of **CU09** (DMSO-d_6)

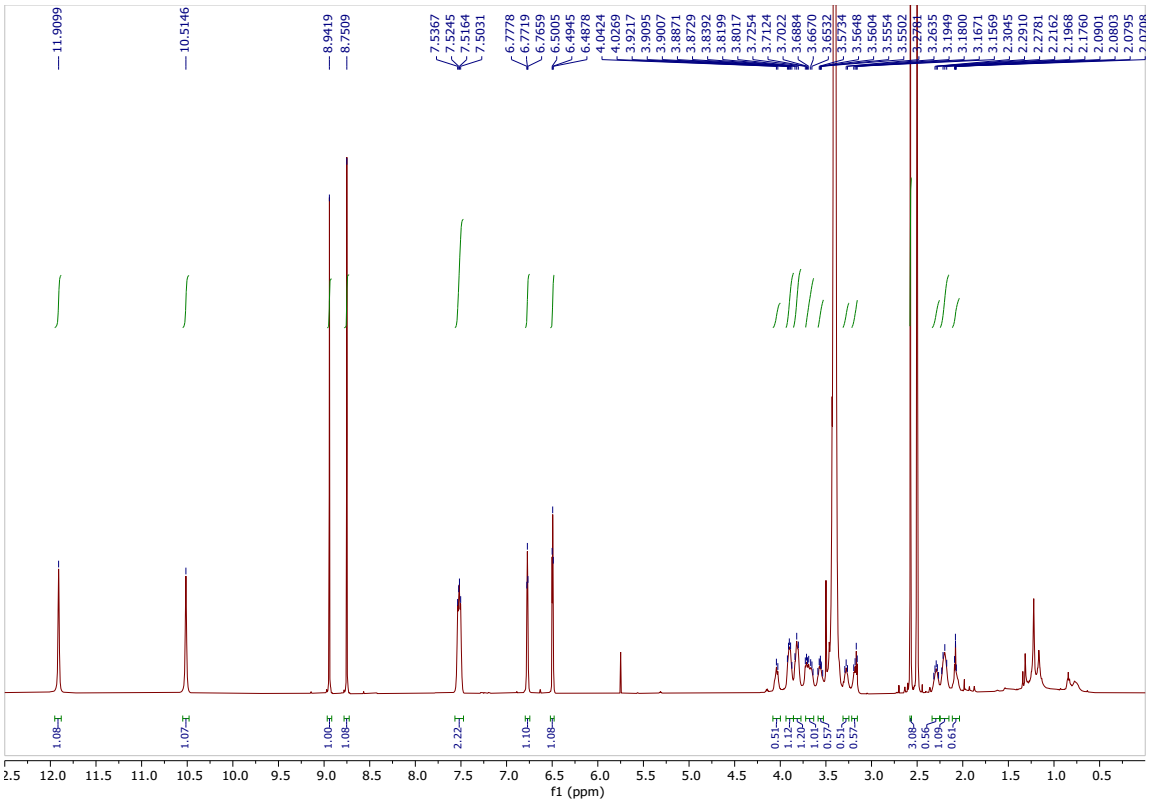

^{1}H NMR spectrum of **CU10** (DMSO-d_6)

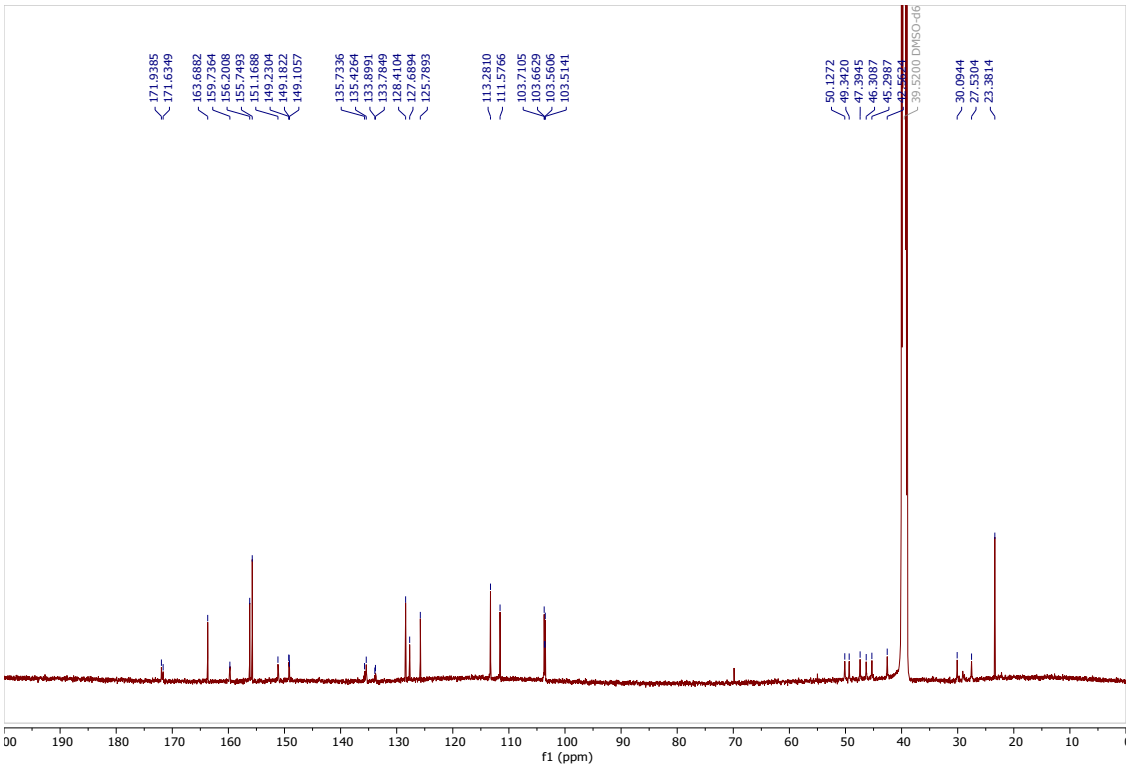

^{13}C NMR spectrum of **CU10** (DMSO-d_6)

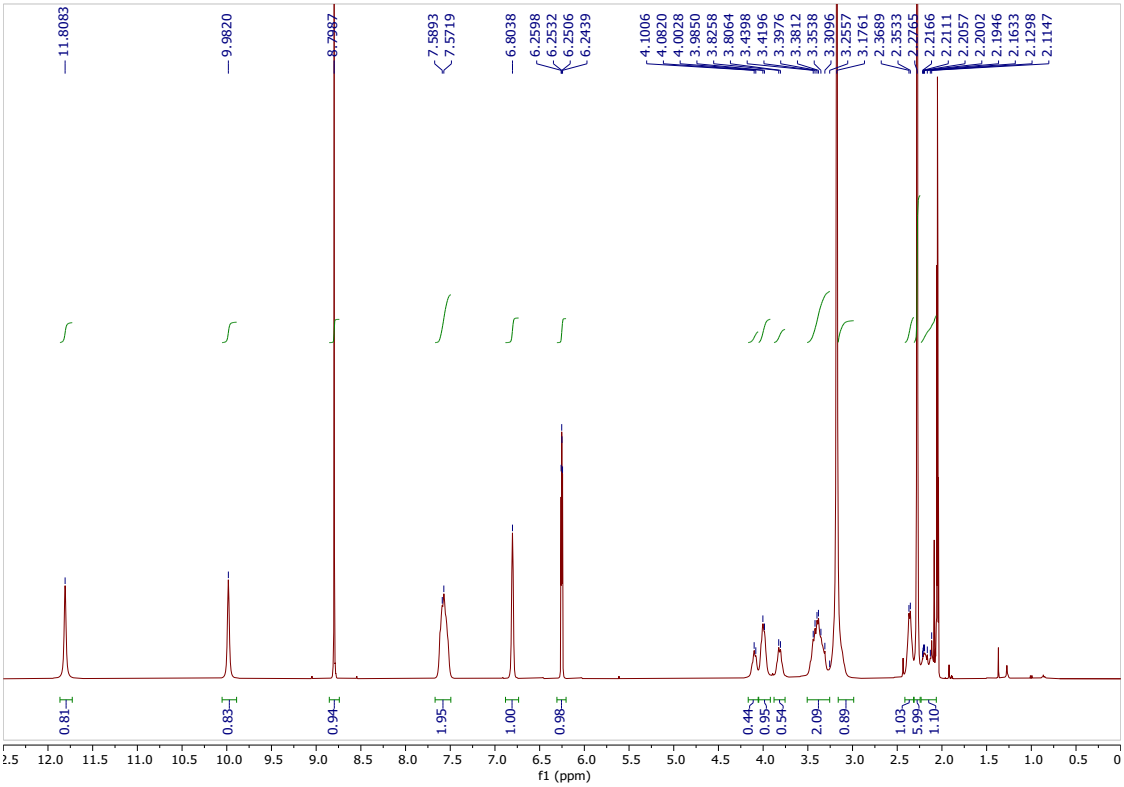

^{1}H NMR spectrum of **CU11** (Acetone-d_6)

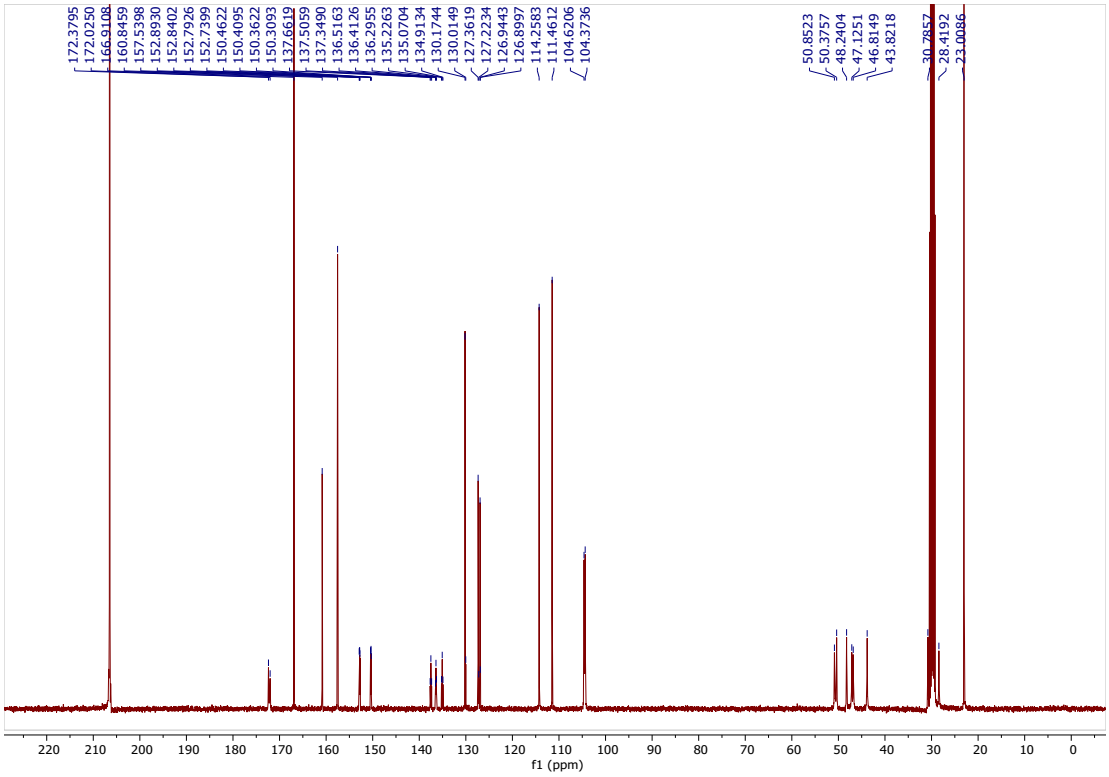

^{13}C NMR spectrum of **CU11** (Acetone-d_6)

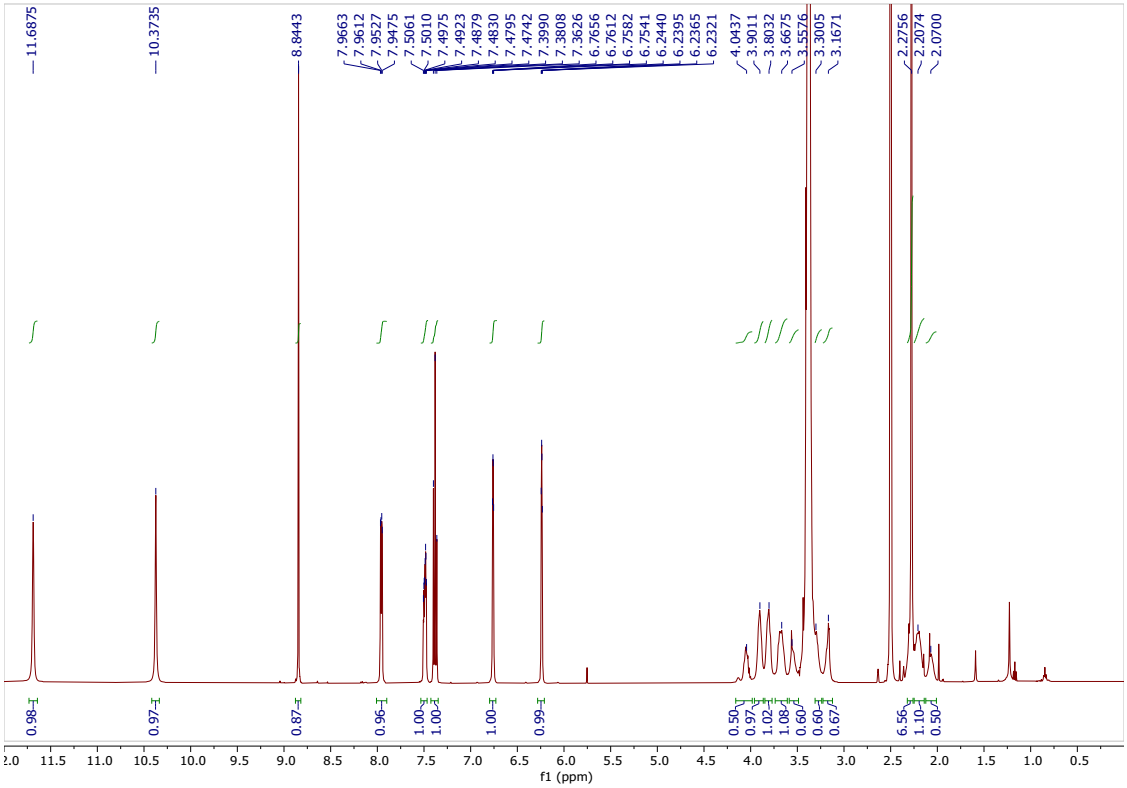

^{1}H NMR spectrum of **CU12** (Acetone-d_6)

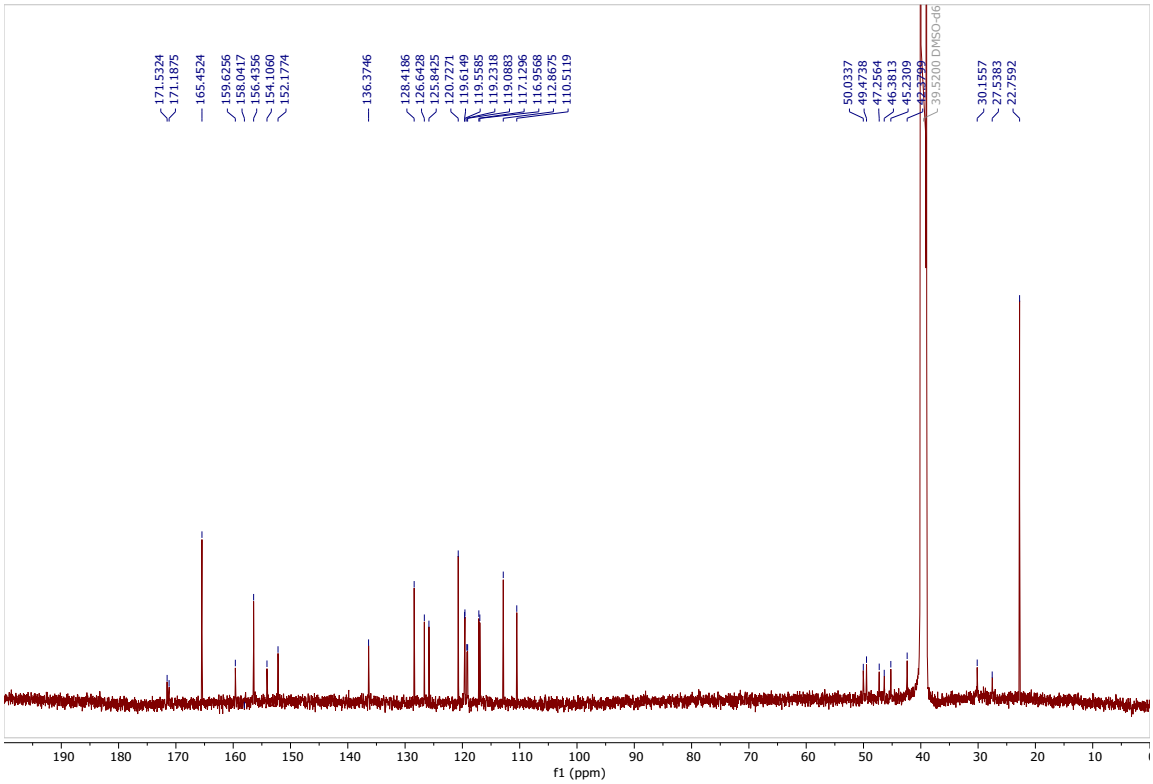

^{13}C NMR spectrum of **CU12** (Acetone-d_6)

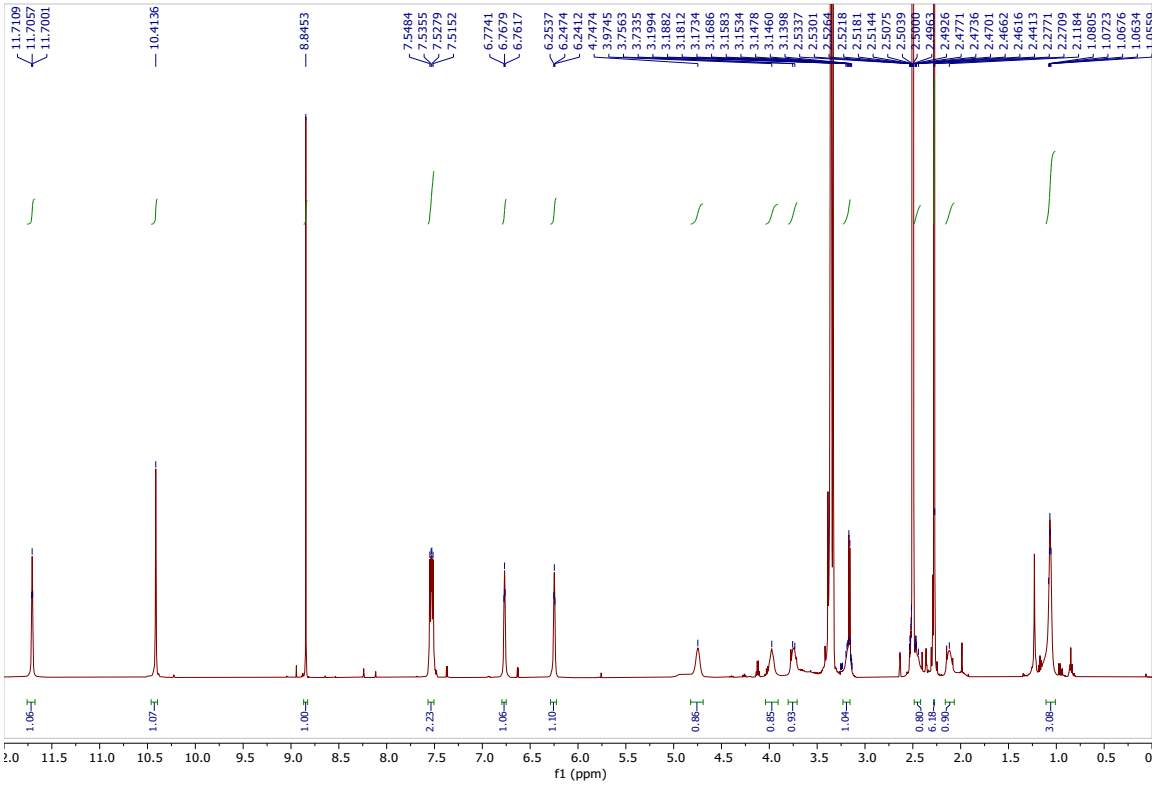

^{1}H NMR spectrum of **CU13** (Acetone-d_6)

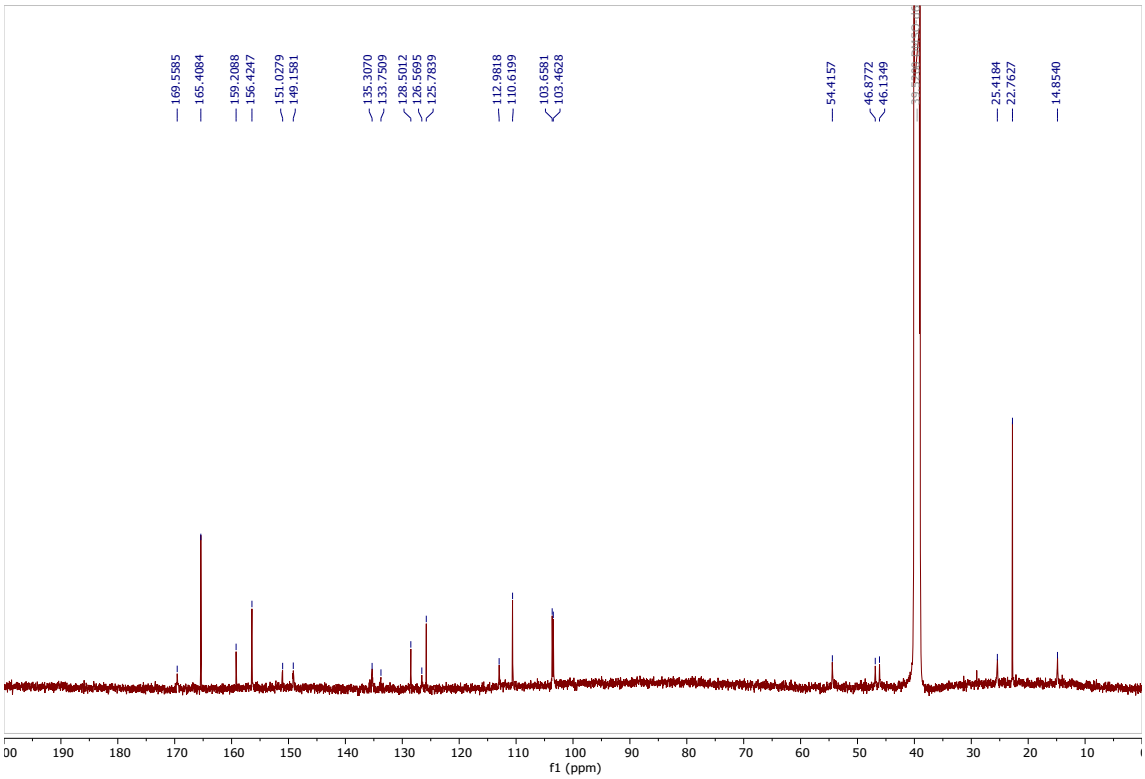

^{13}C NMR spectrum of **CU13** (Acetone-d_6)

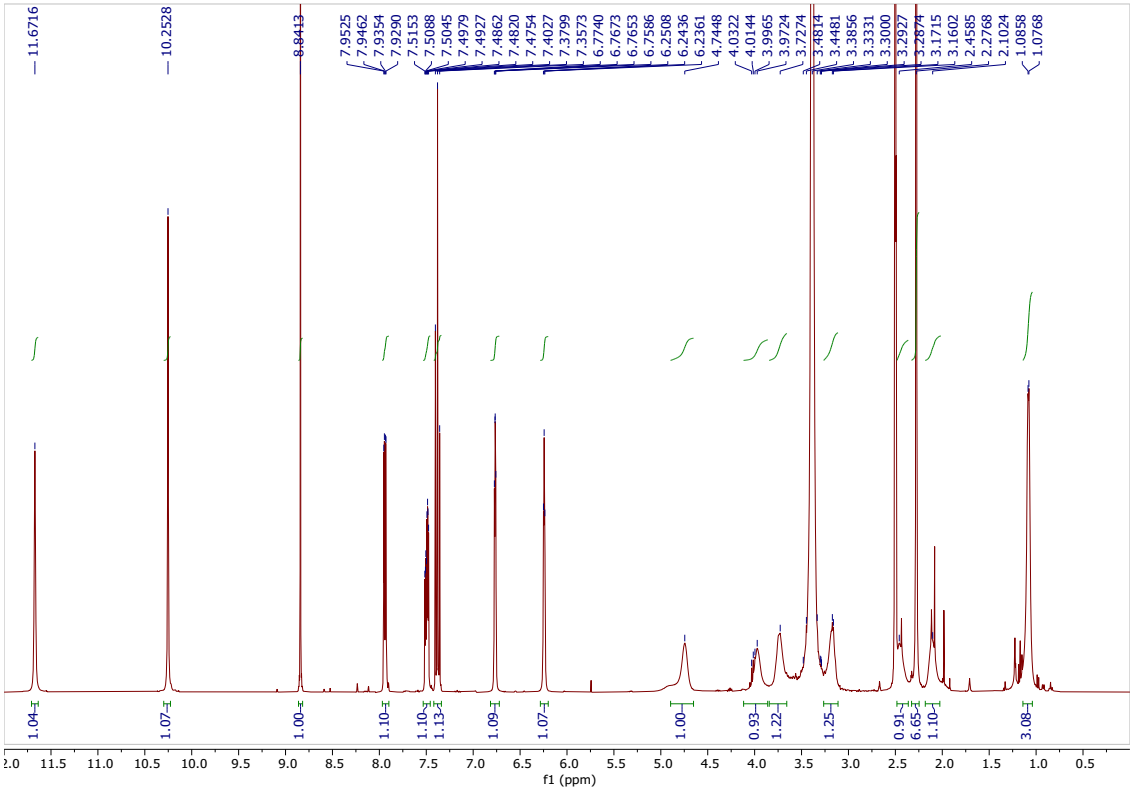

^{1}H NMR spectrum of **CU14** (DMSO-d_6)

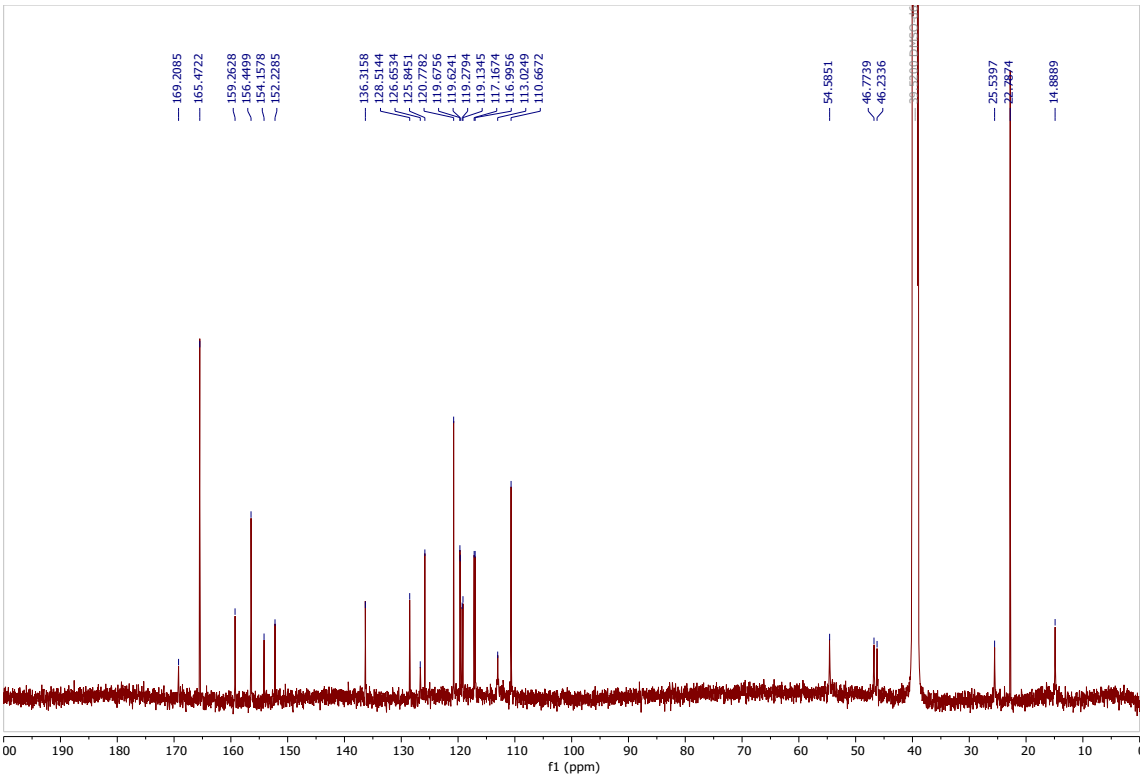

^{13}C NMR spectrum of **CU14** (DMSO-d_6)

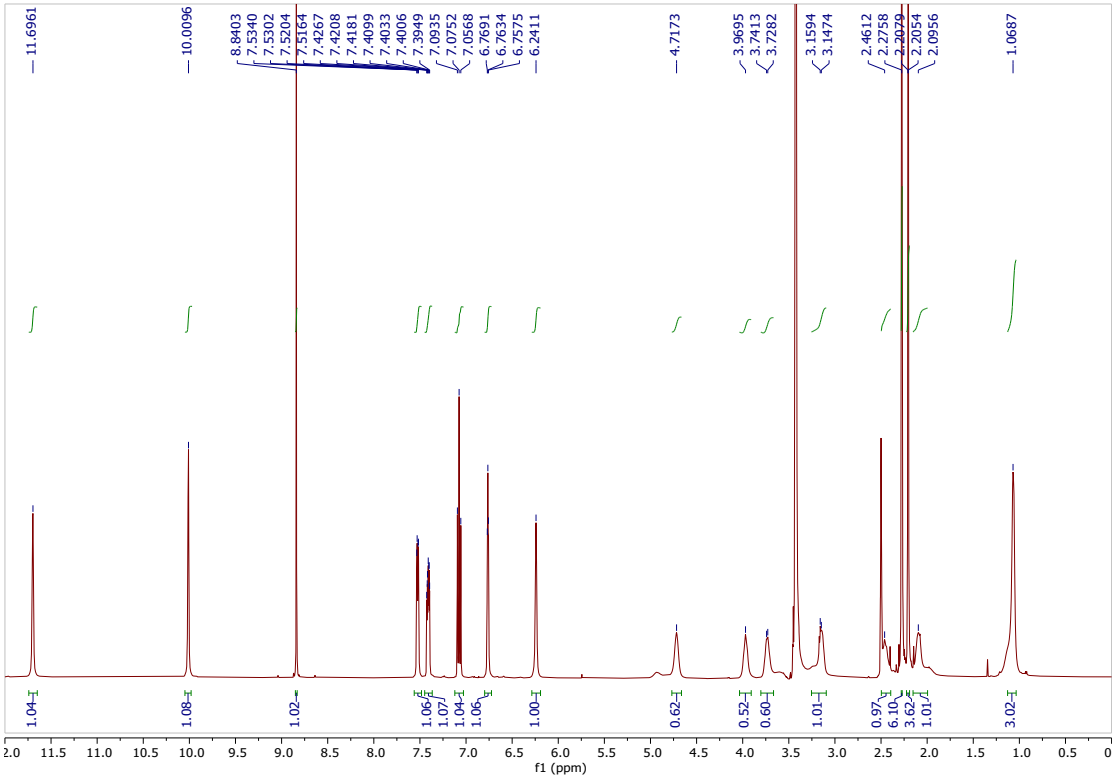

^{1}H NMR spectrum of **CU15** (DMSO-d_6)

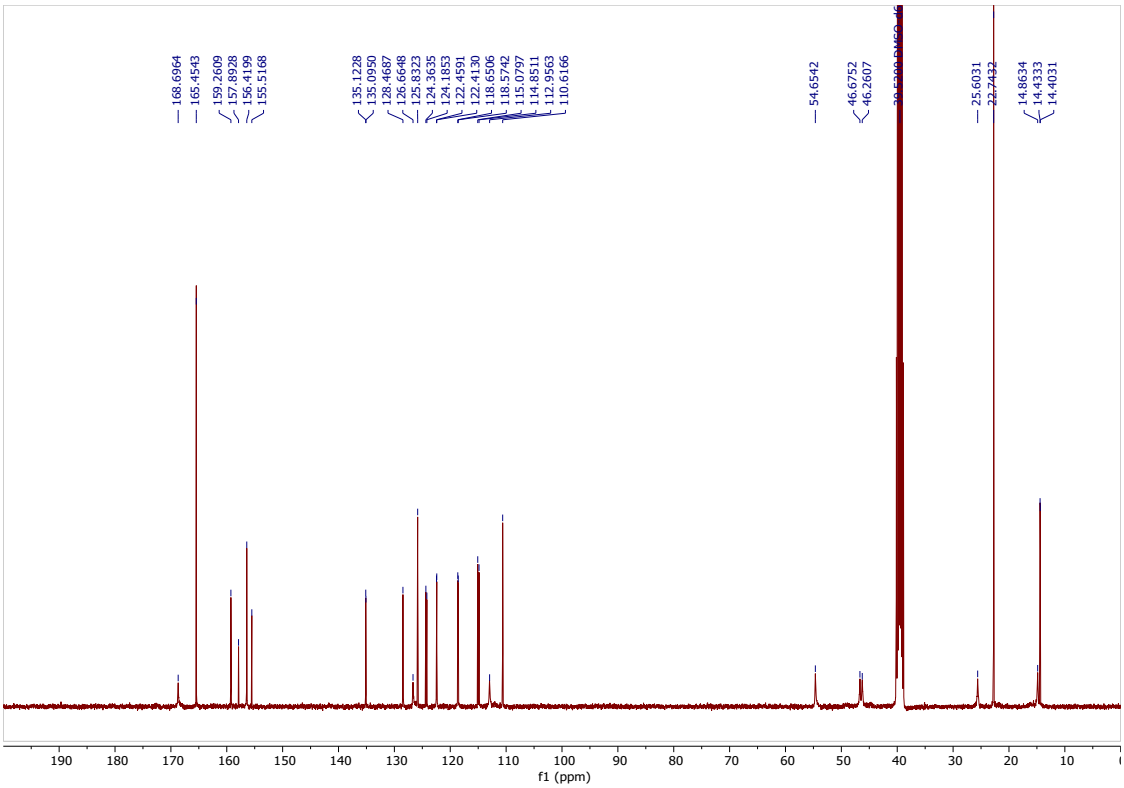

^{13}C NMR spectrum of **CU15** (DMSO-d_6)

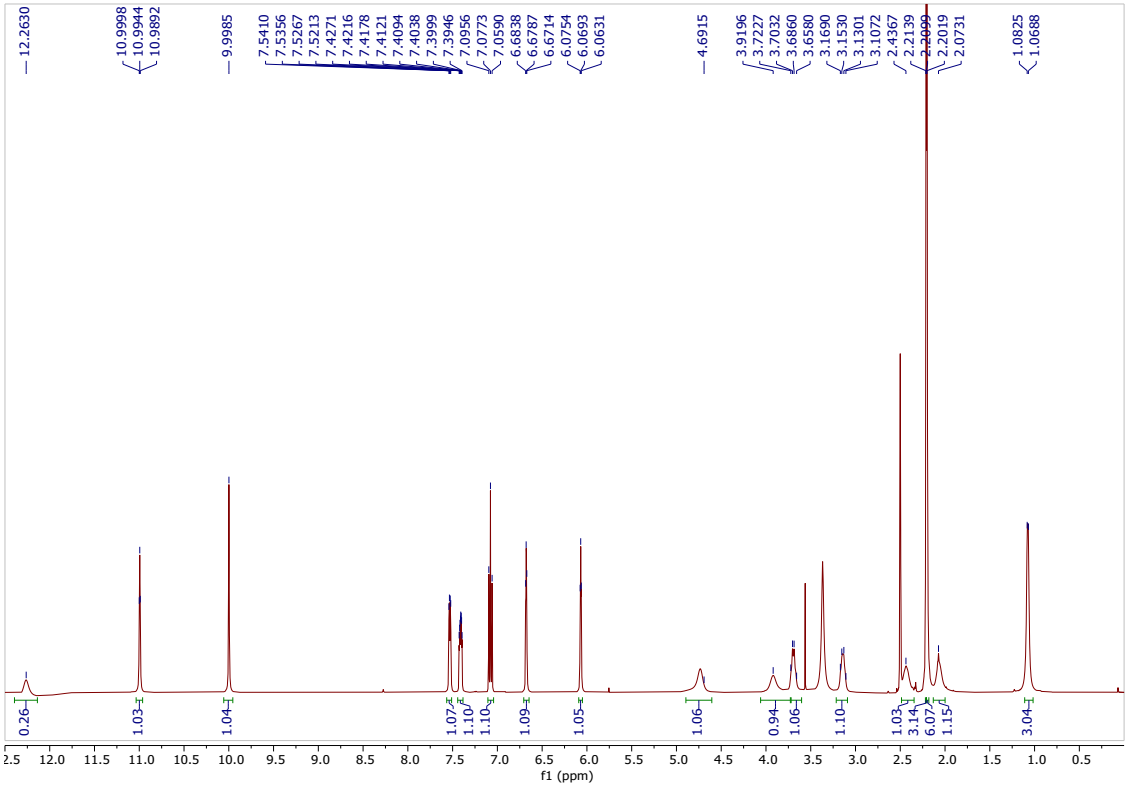

^{1}H NMR spectrum of **CU16** (DMSO-d_6)

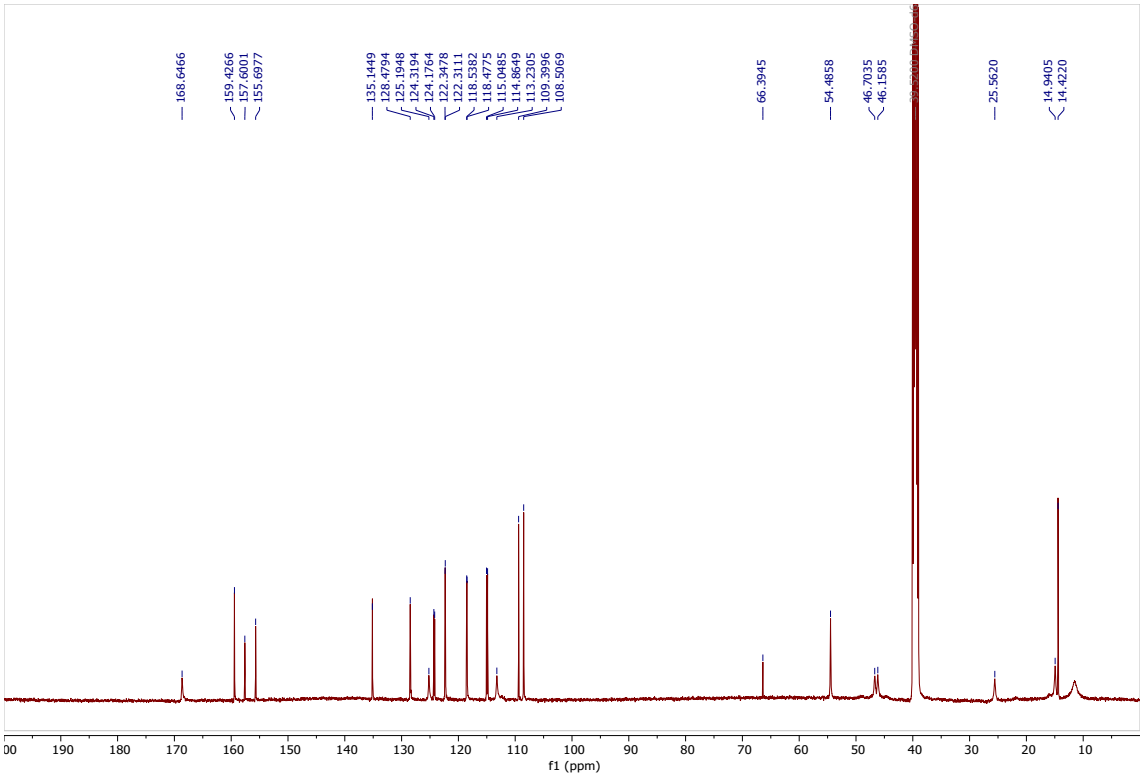

^{13}C NMR spectrum of **CU16** (DMSO-d_6)